Atmos. Chem. Phys. Discuss., 13, 255–309, 2013
www.atmos-chem-phys-discuss.net/13/255/2013/
doi:10.5194/acpd-13-255-2013

Atmospheric Chemistry and Physics Discussions

Multiannual changes of CO_2 emissions in China: indirect estimates derived from satellite measurements of tropospheric NO_2 columns

E. V. Berezin[1], I. B. Konovalov[1], P. Ciais[2], A. Richter[3], S. Tao[4], G. Janssens-Maenhout[5], M. Beekmann[6], and E.-D. Schulze[7]

[1]Institute of Applied Physics, Russian Academy of Sciences, Nizhniy Novgorod, Russia
[2]Laboratoire des Sciences du Climat et l'Environnement (LSCE/IPSL), CNRS-CEA-UVSQ, Centre d'Etudes Orme des Merisiers, Gif sur Yvette, France
[3]Institute of Environmental Physics and Remote Sensing, IUP/IFE, University of Bremen, Bremen, Germany
[4]Laboratory for Earth Surface Processes, College of Urban and Environmental Sciences, Peking University, Beijing 100871, China
[5]Joint Research Center, Institute for Environment and Sustainability, Ispra (Va), Italy
[6]Laboratoire Inter-Universitaire de Systèmes Atmosphériques (LISA/CNRS), CNRS, UMR7583, Université Paris-Est and Université Paris 7, Créteil, France
[7]Max Planck Institute for Biogeochemistry, Jena, Germany

Received: 12 November 2012 – Accepted: 14 December 2012 – Published: 7 January 2013

Correspondence to: I. B. Konovalov (konov@appl.sci-nnov.ru)

Published by Copernicus Publications on behalf of the European Geosciences Union.

Abstract

Multi-annual satellite measurements of tropospheric NO_2 columns are used for evaluation of CO_2 emission changes in China in the period from 1996 to 2008. Indirect annual top-down estimates of CO_2 emissions are derived from the satellite NO_2 columns measurements by means of a simple inverse modeling procedure involving simulations performed with the CHIMERE mesoscale chemistry transport model and the CO_2 to NO_x emission ratios from the Emission Database for Global Atmospheric Research version 4.2 (EDGAR v4.2) global anthropogenic emission inventory. Exponential trends in the normalized time series of annual emission are evaluated separately for the periods from 1996 to 2001 and from 2001 to 2008. The results indicate that the both periods manifest strong positive trends in the CO_2 emissions, and that the trend in the second period was significantly larger than the trend in the first period. Specifically, the trends in the first and second periods are estimated to be in the range from 3.7 to 8.0 and from 9.5 to 13.0 percent per year, respectively, taking into account both statistical and probable systematic uncertainties. Comparison of our top-down estimates of the CO_2 emission changes with the corresponding bottom-up estimates provided by EDGAR v4.2 and Global Carbon Project (GCP) emission inventories reveals that while acceleration of the CO_2 emission growth in the considered period is a common feature of the both kinds of estimates, nonlinearity in the CO_2 emission changes may be strongly exaggerated in the emission inventories. Specifically, the atmospheric NO_2 observations do not confirm the existence of a sharp bend in the emission inventory data time series in the period from 2000 to 2002. A significant quantitative difference is revealed between the bottom-up and top-down estimates of the CO_2 emission trend in the period from 1996 to 2001 (specifically, the trend was not positive according to the emission inventories, but is strongly positive in our estimates). These results confirm the findings of earlier studies which indicated probable large uncertainties in the energy production and other activity data from international energy statistics used as the input information in the emission inventories for China. For the period from 2001 to 2008,

ACPD
13, 255–309, 2013

the different kinds of estimates agree within the uncertainty range. In general, satellite measurements of tropospheric NO_2 are shown to be a useful source of information on CO_2 sources colocated with sources of nitrogen oxides; the corresponding potential of these measurements should be exploited further in future studies.

1 Introduction

The rapid increase in atmospheric carbon dioxide (CO_2) concentration due to anthropogenic emissions is commonly recognized as one of the major driving forces of the global warming (IPCC, 2007). Good knowledge of CO_2 anthropogenic emissions into the atmosphere and their long-term changes is therefore indispensible to any scientific study or science-based policy actions aiming at prediction and control of the climate change.

Presently, CO_2 and other greenhouse gas (GHG) emissions on different temporal and spatial scales are reported in many international (e.g. Olivier et al., 2005; GCP, 2010; Ciais et al., 2010; Janssens-Maenhout et al., 2012) and national (e.g. Ohara et al., 2007; Zhao et al., 2012; Huang et al., 2011) inventories. Such inventories are based on combination of available statistical information on activities in different sectors of the economy (such as transport, industries, energy production, etc.) with emission factors for individual processes and fuel types. There are, however, evidences of inaccuracies in the available statistical information, leading to errors in corresponding emission estimates. For example, Akimoto et al. (2006) and Guan et al. (2012) discuss possible underestimation of fossil fuel CO_2 emissions in China due to inaccuracies in official information on the fossil fuel (in particular, coal) consumption.

An alternative way to obtain emission estimates of CO_2 and other trace gases is provided by the inverse modeling approach (Enting, 2002). Emission estimates derived from trace gas observations by means of atmospheric models can improve knowledge of the GHG balance (e.g. Schulze et al., 2009) and help in pinpointing possible uncertainties and inconsistencies in the bottom-up inventories. For brevity, emissions

ACPD
13, 255–309, 2013

estimates constrained by atmospheric measurements are referred below to as "top-down" estimates, while more traditional emission estimates based on emission inventories are referred to as "bottom-up" estimates.

In the last decade, the inverse modeling approach has rapidly been gaining popularity due to the advent of satellite measurements of various trace gases in the troposphere (Burrows et al., 2011). In particular, satellite measurements of nitrogen dioxide (NO_2) have been widely used to retrieve spatial structure and trends of emissions of nitrogen oxides (e.g. Martin et al., 2003; Müller et al., 2005; Konovalov et al., 2006, 2008; Kurokawa et al., 2009; Wang et al., 2007; Napelenok et al., 2008; Miyazaki et al., 2012); carbon monoxide (CO) measurements were found to be helpful for constraining CO emissions (e.g. Arellano et al., 2004; Pétron et al., 2004; Heald et al., 2004; Kopacz et al., 2010) satellite observations of methane (CH_4) were used to validate and improve CH_4 bottom-up emission estimates (e.g. Bergamaschi et al., 2007, 2009; Monteil et al., 2011). It was also demonstrated (e.g. Curci et al., 2010; Lee et al., 2011; Palmer et al., 2003; Dufour et al., 2009; Millet et al., 2008; Stavrakou et al., 2009) that satellite measurements can provide useful information about emissions of several important organic gases.

Numerous studies (e.g. Rayner and O'Brien, 2001; Pak and Prather, 2001; Houweling et al., 2004; Chevallier et al., 2007; Kadygrov et al., 2009; Hungershoefer et al., 2010; Nassar et al., 2011a,b) studied the potential of satellite CO_2 measurements as a source of information on CO_2 emissions and natural sinks. It has been demonstrated from model studies that inversions of such measurements could facilitate improvements of CO_2 emission estimates on large (continental) scales. At the same time, it has also been found that emission estimates derived from CO_2 satellite observations are especially sensitive to model and measurement errors (e.g. Houweling et al., 2010). This sensitivity reflecting the large life time and relatively small variability (typically, less than 5 percent) of CO_2 columns in the atmosphere seriously hinders estimation of CO_2 emissions and their changes on finer (regional) scales. Similar limitations also exist in the case of CO_2 inversions based on ground based measurements (Enting, 2002),

ACPD
13, 255–309, 2013

with these measurements being more precise but more sparse than the satellite remote sensing data.

One of the promising ideas in this context is estimation of CO_2 fluxes by using measurements of other tracers in situations where the main sources of the tracers and CO_2 are essentially the same (Rivier et al., 2006). This idea was recently exploited, in particular, by Brioude et al. (2012) who used aircraft measurements of several species (CO, NO_y, and SO_2) to estimate CO_2 emissions from Houston. Earlier, Palmer et al. (2006) and Suntharalingam et al. (2004) used the correlation between CO and CO_2 instantaneous observations during aircraft campaigns to improve spatial allocation of CO_2 emission sources in Eastern Asia, including China.

The focus of this paper is the evaluation of multi-annual changes in CO_2 emissions from China, which according to Boden et al. (2011) and other inventories has recently become the world leader in total CO_2 emissions. Our idea is that indirect but still useful information about these changes can be derived from satellite measurements of tropospheric NO_2 columns. Indeed, on the one hand, it was shown earlier that such measurements clearly reflect local "hot spots" and long-term changes in anthropogenic NO_x emissions in China (Richter et al., 2005; Wang et al., 2010, 2012b; Zhang et al., 2007; Lin, 2012). On the other hand, both CO_2 and NO_x have many common sources associated with fossil fuel and other fuel combustion and therefore temporal changes in anthropogenic emissions of these species should be related. Importantly, due to the relatively short lifetime of NO_x, NO_2 atmospheric observations reflect the spatial and temporal structure of emission fields in much more detail than similar CO_2 observations, which are reflecting both long-range transport from distant emissions, and local emissions. To relate NO_x emissions to the NO_2 observations we employ a mesoscale chemistry-transport model and a simple inverse modeling method similar to that used in Konovalov et al. (2010) for studying NO_x emission trends in megacities. The assumed relation between CO_2 and NO_x emission is specified using data of emission cadastres.

ACPD
13, 255–309, 2013

Since CO_2 emission trend estimates obtained in this study are based on observations (even though some emission inventory data are also involved), they are to a significant extent independent from similar estimates provided by emission inventories. Taking this into account, we believe that our top-down CO_2 emission estimates can be helpful for detecting and elucidating possible uncertainties and/or inconsistencies in alternative bottom-up emission estimates and in inventory data which are used to relate NO_x and CO_2 emissions in our analysis. Specifically, a disagreement between the top-down and bottom-up estimates in our case may indicate (assuming that our estimates of NO_x emissions are sufficiently accurate) that either the inventory data for CO_2 emissions or the assumed relationship between CO_2 and NO_x emissions (the NO_x to CO_2 emission conversion factor) or both are insufficiently accurate. Note that we did not evaluate absolute values of NO_x or CO_2 emissions from China; only their temporal changes from a baseline year value are examined here. Due to this, our results are expected to be rather insensitive to poorly known biases in the modeled and measured NO_2 columns, as long as these biases remain constant with time during the study period.

The data used in our analysis are described in Sect. 2. The method is outlined in Sect. 3. Our estimates of CO_2 and NO_x emission trends in China are presented in comparison with corresponding data of several emission inventories in Sect. 4. The potential uncertainties of our results and their possible implications are discussed in Sect. 5. Finally, main findings of this study are summarized in Sect. 6.

2 Data

2.1 Data of satellite measurements

We used tropospheric NO_2 column amounts retrieved as described by Richter et al. (2005) at the Institute of Environmental Physics and Remote Sensing, University of Bremen from measurements performed by the GOME (1996–2002) (Burrows

ACPD
13, 255–309, 2013

et al., 1999) and SCIAMACHY (2003–2008) (Bovensmann et al., 1999) instruments onboard the ERS-2 and ENVISAT satellites, respectively. Specifically, we used the standard monthly data products (GOME tropospheric excess NO_2 columns Version 2 (Nüß, 2005) and SCIAMACHY tropospheric excess NO_2 columns Version 0.7 (Richter et al., 2005) provided on a regular grid with the resolution of $0.5 \times 0.5^{\circ}$ and $0.125 \times 0.125^{\circ}$ in the cases of GOME and SCIAMACHY data, respectively. The same data were already used in several previous studies aimed at evaluation of long-term changes of NO_x emissions in different regions of the world (Richter et al., 2005; He et al., 2007; Kim et al., 2006, 2009; Konovalov et al., 2008, 2010). The initial nominal horizontal resolution of the GOME measurements is $320 \times 40\,km^2$, and almost global coverage is achieved within 3 days. The SCIAMACHY measurements have a higher nominal horizontal resolution of $60 \times 30\,km^2$, but at the expense of a longer global coverage period of about 6 days.

Preprocessing of the "standard" monthly datasets included several steps described below. First, the global data were re-gridded to a 0.5 by 0.5 degree regional grid focusing on China. Second, "empty" grid cells (in which measurements are missing, e.g. because of clouds) in each of the monthly datasets were filled in by means of a temporal or spatial interpolation. Specifically, an empty grid cell in a given monthly dataset was assigned with either the average over the two nearest months or (if the data for those months are also missing) the average over the eight closest grid cells of the same month. Finally, to ensure the consistency of NO_2 columns measured with different spatial resolution, the SCIAMACHY data were spatially smoothed on the longitudinal plane in the same way as in Konovalov et al. (2010) to simulate the smoothing introduced by the GOME measurements. Specifically, the smoothed c^{s} and original c^{or} NO_2 columns

ACPD
13, 255–309, 2013

are related as follows:

$$c^{s}_{(i)} = \sum_{j=0}^{2m} c^{or}_{i-m+j}\rho_j \left[\sum_{k=0}^{2m}\rho_k\right]^{-1},$$

$$\rho_j = \exp\left[-\frac{1}{2}\left(\frac{(j-m)\cos(\varphi)}{\lambda}\right)^2\right] \quad (1)$$

where the lower subscripts specify the longitudinal grid cell index (counting along a constant latitude); m is the number of grid cells on the longitudinal plane within 320 km (the typical resolution of the GOME measurements), φ is the latitude, and λ is the effective distance scale. The value of λ was estimated in Konovalov et al. (2010) to be of 0.85 ± 0.16 by minimizing the mean squared difference between the smoothed NO_2 columns (from SCIAMACHY) for 2003 and the original NO_2 columns (from GOME) for 2002 over 12 urban agglomerations situated in Europe and in the Mediterranean. Note that our results concerning total emissions from a very large region (such as the eastern part of China) considered in this study are found to be quite insensitive to the choice of value of λ. As it was shown previously (Richter et al., 2005), the GOME and SCIAMACHY data averaged over the eastern part of China are sufficiently consistent (even without smoothing of the SCIAMACHY data) and their combined time series can therefore be used for evaluation of corresponding emission changes. The smoothing procedure involving a sufficiently accurate estimate of λ is however more important when emissions from smaller regions (such as China's provinces) are evaluated.

2.2 Data of emission inventories

We used annual emission data from several emission databases, including the Emission Database for Global Atmospheric Research, version 4.2 (EDGAR v4.2), the Global Carbon Project (GCP) international databases and a new global data product for CO_2 emission by combustion processes (PKU-CO2) compiled at the Peking University. CO_2

ACPD
13, 255–309, 2013

and NO_x emissions are available from the EDGAR v4.2 (EC-JCR/PBL, 2010) database both as the national totals and on a grid with the resolution of 0.1 by 0.1 degrees. GCP (GCP, 2010) provides only total national carbon emission estimates. The Peking University (PKU-CO2) emission inventory (Wang et al., 2012a) consists of gridded CO_2 emissions from combustion processes over the globe, using county level fuel data in China. The data from the EDGAR v4.2 gridded and GCP country-averaged emission inventories covers the whole period addressed in this study (1996–2008), while the PKU-CO2 inventory was established for the year 2007, and updated with the new county-level data in China for three years only (1997, 2002 and 2008) in this study.

The methods used in the EDGAR and GCP emission inventories are described in detail elsewhere (e.g. Olivier et al., 2001; Ciais et al., 2010; Janssens-Maenhout, 2012). The PKU-CO2 emission inventory with detailed fuel categories is based on a sub-national disaggregation approach using sub-national fuel consumption data for large countries. Details can be found elsewhere (Wang et al., 2012a).

2.3 Simulated data

To evaluate the relationship between the tropospheric NO_2 columns and NO_x emissions, we used the CHIMERE chemistry transport model (www.lmd.polytechnique.fr/chimere). CHIMERE is a mesoscale Eulerian three-dimensional model which takes into account all important processes determining the evolution of nitrogen oxides in the troposphere, such as a number of gas phase and heterogeneous chemical reactions, dry and wet deposition, advection, turbulent diffusion and deep convection. Parameterizations of these processes in the model are described in several papers (e.g. Schmidt et al., 2001; Bessagnet et al., 2004; Hodzic and Jimenez, 2011).

The simulations were performed with a horizontal resolution of $1^\circ \times 1^\circ$ for 12 layers in the vertical (up to 200 hPa pressure level). The model domain covered the East Asia region (from 58.250° to 141.750° E and from 20.250° to 65.750° N) including continental China. Meteorological data were obtained from the WRF-ARW model (Skamarock et al., 2005; Wicker and Scamarock, 2002) which was run with a horizontal resolution

ACPD
13, 255–309, 2013

of $90 \times 90\,km^2$ and driven with the NCEP Reanalysis-2 data. Chemical processes were simulated with the MELCHIOR1 chemical mechanism, including about 300 reactions of 80 model species. Boundary conditions for gases and aerosols were taken from climatological runs of LMDZ (Lott et al., 2005; Hourdin et al., 2006) and GOCART (Ginoux et al., 2001; Chin et al., 2000, 2002), respectively. Anthropogenic emissions were specified using the EDGAR v4.1 data, biogenic emissions were based on the MEGAN global inventory (Guenther et al., 2012). Note that since the model is used here only for evaluation of the NO_x lifetime, some differences between the latest version (v4.2) of the EDGAR inventory (which was not available when the simulations were performed) and its previous version (v4.1) are unimportant in this context. Along with the "baseline" scenario where both anthropogenic and biogenic emissions were taken into account, the model was also run with zero anthropogenic emissions in China.

In order to be consistent with satellite data, which are described in Sect. 2.1, the modelled NO_2 columns for each model grid cell are taken between 10 and 12 h of local solar time and only on days with insignificant cloud cover. Since the total cloud cover was not used in the CHIMERE simulation, we use a selection criteria based on threshold value of the radiation attenuation coefficient. Specifically, we disregarded days on which reduction of solar radiation due to clouds was larger than 30 percent. The same criterion was used in our earlier studies (Konovalov et al., 2005, 2006). The simulated NO_2 columns were smoothed in the same way as the SCIAMACHY data.

Figure 1 presents the spatial distributions of the simulated and measured NO_2 columns over China (before smoothing). It can be seen that CHIMERE reproduces the data derived from satellite measurements rather adequately, although the agreement is obviously not perfect. In particular, the model systematically underestimates the NO_2 columns over the most polluted industrial regions in the eastern part of China. Systematic underestimation of satellite measurements of NO_2 columns over China by simulations was found earlier in other studies employing different models and emission data (e.g. Ma et al., 2006; He et al., 2007; Lin et al., 2010; Lin, 2012). Such underestimation is likely due to a corresponding bias in NO_x emission inventories for China, but

ACPD
13, 255–309, 2013

it also may be in part due to some systematic chemistry-transport model and measurement errors.

3 Method

The first step of our method is the estimation of interannual changes in anthropogenic NO_x emissions. Similar to many previous studies (e.g. Martin et al., 2003; Konovalov et al., 2006; Wang et al., 2007; Ghude et al., 2008; Lin et al., 2010; Lin, 2012) we assume that the relationship between NO_2 column concentrations and NO_x emissions is linear. Following Konovalov et al. (2010), we define:

$$C_i \approx \alpha_i E_i^{(NO_x)} + C_{bi}, \quad (2)$$

where C_i is the monthly mean total tropospheric NO_2 column amount over a considered region for the month i; $E_i^{(NO_x)}$ is the corresponding anthropogenic NO_x amount emitted in the same region and month, α_i is the sensitivity of the NO_2 columns to changes of the NO_x emissions, and C_{bi} is the "background" level of the tropospheric NO_2 column amounts, which is not related to anthropogenic emissions in the given region and month. Note that α_i can be interpreted as the effective lifetime of NO_2 columns with regard to both chemical and transport processes.

Estimates of α_i can be derived from model results for the special scenario where seasonal (monthly) variation of emissions is absent. Similar to Eq. (2) we can define:

$$C_{0i} \approx \alpha_i E_0^{(NO_x)} + C_{bi}, \quad (3)$$

where $E_0^{(NO_x)}$ is the constant NO_x monthly anthropogenic emission specified in the model. After expressing α_i from Eq. (3) and substituting it into Eq. (2) we get:

$$E_i^{(NO_x)} / E_0^{(NO_x)} = \frac{C_i - C_{bi}}{C_{0i} - C_{bi}} \quad (4)$$

ACPD
13, 255–309, 2013

Using Eq. (4), the total annual emission, $E_t^{(NO_x)}$, in the same region can be expressed as follows:

$$E_t^{(NO_x)}/E_0^{(NO_x)} \approx \sum_{i=1}^{12} \left(\frac{C_i - C_{bi}}{C_{0i} - C_{bi}} \right). \quad (5)$$

To estimate annual combustion CO_2 emissions, $E_t^{(CO_2)}$, from the NO_x emissions, we define the average NO_x-to-CO_2 emission conversion factor (for a given year and an area) as

$$F = E_t^{(CO_2)}/E_t^{(NO_x)}. \quad (6)$$

Taking Eqs. (5) and (6) into account, the ratio of CO_2 emissions in two different years can be estimated as follows:

$$E_t^{(CO_2)j}/E_t^{(CO_2)k} \approx F^j \sum_{i=1}^{12} \left(\frac{C_i^j - C_{bi}^j}{C_{0i}^k - C_{bi}^k} \right) / F^k \sum_{i=1}^{12} \left(\frac{C_i^k - C_{bi}^k}{C_{0i}^k - C_{bi}^k} \right), \quad (7)$$

where the upper indexes (j and k) denote years. A similar relationship (with $F = 1$) can be used to estimate the relative changes in NO_x emission. Here and below the bold italicized character $\boldsymbol{F}$ denotes a vector whose components are values of the NO_x-to-CO_2 emission conversion factor for different years. We also use below the bold characters $\mathbf{C}$, $\mathbf{C}_0$ and $\mathbf{C}_b$ to denote matrices containing monthly values of the corresponding characteristics (defined above) for different years. By fixing a value of k, we define a reference year and obtain time series of NO_x and CO_2 emissions related to those in the reference year. Our final goal is the independent evaluation of combustion CO_2 emission trends by means of different approximations of the relative annual CO_2 emission estimates specified by Eq. (7).

ACPD
13, 255–309, 2013

In this study, estimates of the emission factors are prescribed from the EDGAR v4.2 inventory; the behavior of the emissions factors along with the evolution of the corresponding total NO_x and CO_2 emissions in China in the period from 1996 to 2008 are presented in Fig. 2. It is noteworthy that according to EDGAR v4.2 the long-term changes in the NO_x and CO_2 emissions are rather similar (especially before 2003). This fact illustrates the usefulness of considering NO_x emissions as a proxy for CO_2 emissions. Some deviation in the NO_x and CO_2 emission changes after 2003 is mainly due to the introduction of NO_x emissions abatement measures (catalytic reduction or combustion modification), as reported e.g. by Zhang et al. (2007).

Values of $\mathbf{C}_0$ and $\mathbf{C}_b$ are evaluated by means of the CHIMERE chemistry transport model under the following assumptions:

1. the impact of NO_x emitted in a previous month on the NO_2 columns in a given month is negligible (note that in principle this impact could be reflected in $\mathbf{C}_b$);
2. the transport of NO_x into a considered region from outside is also negligible;
3. the long-term changes in natural NO_x emissions (from soil, wildfires and lightning) are much smaller than the trends in anthropogenic emissions and can be disregarded;
4. the impact of interannual changes in $\mathbf{C}_0$ and $\mathbf{C}_b$ due to meteorological variability and other factors (such as trends in emissions of volatile organic compounds (VOC)) on the NO_x emission estimates derived in accordance to Eq. (7) is small (in particular, in comparison with the impact of uncertainties in the measured and modeled NO_2 columns) and can also be disregarded.

These assumptions, which, in our opinion, are sufficiently reasonable and justifiable (see Sect. 5) in view of results of numerous previous studies employing satellite NO_2 measurements, allowed us to get sufficiently accurate estimates of $\mathbf{C}_0$ and $\mathbf{C}_b$ in a computationally efficient way. In particular, we have avoided multi-annual simulations which would be computationally too expensive in our case. Taking these assumptions into

ACPD
13, 255–309, 2013

account, $\mathbf{C}_0$ is calculated in one year-around model run with both anthropogenic and biogenic emissions. Meteorological data were taken for the year 2007. It is essential that such a simulation is done without seasonal variation of the anthropogenic NO_x emissions; the seasonal cycle of the real anthropogenic NO_x emissions in the given region is then "automatically" taken into account in the satellite measurement inversions defined by Eq. 5 and 7. Indeed, if the simulations and measurement data are correct, then any differences in values of the fractions in the right-hand parts of these equations may only be due to corresponding seasonal changes in NO_x emissions.

Note that in addition to the assumption listed above, our simulations do not take into account NO_x emissions from lightning and wildfires. The potential impact of these emissions on our estimates is also discussed in Sect. 5. Note also that in contrast to emissions from wildfires, NO_x and CO_2 emissions from agricultural biomass burning are taken into account in the EDGAR inventory (as the sector 4F) and in our simulations.

The Eqs. (5) and (7) employed in the context of the assumptions listed above constitute the base case (case I) of our estimation method. The emission estimates inferred in this way depend on the assumed seasonal variations of the NO_x lifetime which are implicitly evaluated by the chemistry-transport model. However, as it is discussed below in Sect. 4.1, our evaluation yields stronger seasonal variation of anthropogenic emissions than suggested by "bottom-up" emission inventories, and the possibility that this difference is due to some model uncertainties cannot be definitely ruled out. Accordingly, to take into account possible effects of these uncertainties on our emission trend estimates we consider additional cases (cases II and III) of our estimation method.

Specifically, to assess the impact of the background NO_2 columns on our estimates we consider a hypothetical case (case II) where $\mathbf{C}_b$ in Eq. (7) is set to be zero. Effectively, this case also addresses a situation where the relative changes in the background part of the measured NO_2 columns are the same as the relative changes in their anthropogenic part (including both seasonal and multi-annual changes). The case III is specified in the same way as the case II except that the seasonal variation in the

ACPD
13, 255–309, 2013

measured NO_2 column amounts in a reference year is assumed to be entirely due to a corresponding variation in the NO_x lifetime. To satisfy this assumption, the seasonal variation of $\mathbf{C}_0$ in the formulations discussed above is replaced with $\mathbf{C}$ for the reference year. Accordingly, instead of Eq. (7) we obtain in such a case:

$$E_t^{(CO_2)j} / E_t^{(CO_2)k} \approx \frac{F^j}{12F^k} \sum_{i=1}^{12} \left(\frac{C_i^j}{C_i^k} \right). \quad (8)$$

Unlike estimates provided by Eq. (7), the trends derived from Eq. (8) may be sensitive to the choice of the reference year. This sensitivity is however found to be rather small (in comparison with statistical uncertainties of the trends). For definiteness, we choose $k = 1996$.

Taking into account the character and magnitudes of possible uncertainties in simulated and measured data (see Sect. 5) we believe that such defined three variants of our estimation procedure provide both the upper and lower limits for realistic estimates of the NO_x emission changes. We expect also that the true emission changes should be much closer to our estimates obtained for the case I than to those obtained for the cases II and III of our method.

To evaluate emission trends, we built exponential approximations ($A\exp(kt)$), where A and k are the optimized parameters of the fits, and t is time in years) independently for two periods: 1996–2001 and 2001–2008. These two periods were chosen taking into account a sharp bend in the time series of the EDGAR v4.2 emissions for China (see Fig. 2) between 2000 and 2002. The uncertainty of the exponential trends was estimated with the 95 percent confidence level under the typical assumption that deviations from the approximations satisfy the normal distribution. Note that while using an exponential approximation, we assume that a relative rate of actual emission changes is nearly constant. This rate (in units of percent per year) is estimated as a value of the coefficient k. Such estimation is valid in our case since the obtained values of k are much smaller than unity.

ACPD
13, 255–309, 2013

4 Results

4.1 Quantitative analysis of multiannual emission trends

Our estimates presented in this subsection address a large region (see Fig. 3a) covering the eastern industrial provinces of China and providing (according to EDGAR v4.2) more than 98 percent of the total anthropogenic CO_2 emissions in China. The definition of the region was based on the administrative provincial map of China, so that it includes 27 out of 32 provinces. We selected all provinces where the annual mean and spatially averaged tropospheric NO_2 columns retrieved from the SCIAMACHY measurements in 2008 exceed a threshold value ($[NO_2]_c$) of 10^{15} molecules cm^{-2}. Such a selection allowed us to disregard the provinces where the anthropogenic contribution to the NO_2 columns is too small compared to contributions of natural factors and where, due to that, our emission estimates would be too uncertain.

The top-down estimates of the multi-annual trends in CO_2 emissions (see Eq. 7) are presented in Fig. 4 in comparison with corresponding bottom-up CO_2 emission data of the EDGAR v4.2, GCP and PKU-CO2 emission inventories. It can be seen that while the EDGAR v4.2 and GCP emission inventories demonstrate zero trends (insignificant negative tendencies) in the period from 1996 to 2001, our estimates in all the cases considered show a strong and significant positive trend (specifically, 6.8 ± 1.2 percent per year in the case I). In the second period (from 2001 to 2008), all the bottom-up estimates and the top-down one show large positive trends. Our baseline estimates indicate that the increase of CO_2 emissions in China (12.1 ± 0.9 percent per year in the case I) during this period was almost twice as large as that in the previous period. The trend in the bottom-up emission inventories falls into the range of divergence of different top-down estimates. It may be noteworthy that the trends estimated for the case III are only insignificantly different from those estimated for the case II. This means that the estimated lower limit for the CO_2 emission trends is insensitive to possible uncertainties in the simulated seasonal variation of NO_2 columns.

ACPD
13, 255–309, 2013

Note that qualitatively similar results were found with linear approximation of the trends (not shown). Moreover, we found that linear and exponential trend lines are almost indistinguishable. It should be kept in mind that only relative changes rather than absolute values of emissions are evaluated in this study. Although the differences between relative changes of emissions are inevitably associated with a deviation in absolute values (as it is evident in Fig. 4), the deviation in absolute values cannot be unambiguously attributed to certain years. For example, according to our results the bottom-up CO_2 emissions may, in principle, be quite accurate in 2008 but overestimated in earlier years. It is equally possible that they may be accurate in 1996 and underestimated in later years.

The important result of our analysis is that satellite measurements confirm the accelerating and nonlinear CO_2 emission trend in China, which is manifested by emission inventory data. However, our analysis also reveals strong quantitative differences between the top-down and bottom-up emission estimates for the first time period evaluated. These differences may be indicative of important flaws in the emission inventories. Specifically, the differences between the top-down and bottom-up estimates may be due to a major uncertainty in activity data (annual fuel statistics, industrial production statistics etc.), uncertainty in emission factors, uncertainty in control abatement and uncertainty in spatial distribution assumed in the EDGAR v4.2 inventory for NO_x and CO_2 emissions.

To clarify major factors contributing to our estimates of CO_2 emission trends, we have performed a similar analysis but in the case of NO_x emissions. The measurement-based estimates of NO_x emissions are obtained using the same formulations as our estimates of CO_2 emissions, but with $F = 1$. In parallel, we have evaluated trends directly in the measured NO_2 columns, separately in the cold (1 November–31 March) and warm (1 May–30 September) seasons (these seasons are referred below for brevity to as winter and summer, respectively). The results are shown in Fig. 5. It can be seen that the behavior of the top-down and bottom-up estimates of NO_x emissions is qualitatively and even quantitatively (taking into account uncertainty of the trends) similar

ACPD
13, 255–309, 2013

to the behavior of the respective estimates of CO_2 emissions presented in Fig. 4. This is an expected result, taking into account the assumed behavior of the conversion factor (see Fig. 2) discussed above. It is noteworthy that although the difference between the trends estimated with and without taking into account the background level of NO_2 columns (that is, the difference between the cases I and II) is rather considerable, both kinds of measurement-based estimates demonstrate that the satellite data constrained trends are statistically different from the corresponding trends of the EDGAR v4.2 NO_x emissions in the period from 1996 to 2001.

Interestingly, the measured NO_2 columns demonstrate considerably different behaviors in winter and summer. Specifically, the trends in the NO_2 columns for the cold season are much larger when compared to those for the warm season. Taking into account seasonal variations in the measured and simulated NO_2 columns (see Fig. 6a), our most plausible explanation for this difference is that the slower growth of the NO_2 columns in summer reflects a significant contribution of biogenic emissions (which probably do not experience any significant trends, see also Sect. 5) to the tropospheric NO_2 columns during the warm season. On the other hand, a faster growth of the NO_2 columns in winter may, in principle, reflect an increase of NO_x emissions from the heat production, in particular in the residential sector, while the slower growth of the NO_2 columns in summer is due to larger contribution of NO_x emissions from road transport. However, according to EDGAR v4.2 the road transport sector demonstrates much stronger growing trend than the residential sector and almost the same trend as the public electricity and heat production sector (see also discussion in Sect. 4.2). Finally, one more hypothetical explanation for the differences between the trends in summer and winter is that in winter, the NO_2 lifetime has increased more rapidly than in summer over the time period considered, leading to larger ratios of NO_2 columns to NO_x emissions and larger increases in NO_2 columns in winter than in summer. This explanation is, however, not corroborated by direct simulations with CHIMERE (see Sect. 5).

ACPD
13, 255–309, 2013

As it is noted above, the contribution of different months to annual emissions and their trends is estimated in the framework of our method taking into account possible seasonal variation of both the NO_x lifetime and the background NO_2 level. The seasonal cycles of NO_x emissions for the years 1997 and 2007 estimated in the base case (case I) and in the additional test case (case II) of our method are shown in Fig. 6b. The anthropogenic NO_x emissions are estimated in both cases to be considerably larger in winter than in summer. Specifically, the ratio of the maximum and minimum monthly NO_x emissions is found to be of 3.6 and 1.7 in 1997 and 3.4 and 2.7 in 2007 in the cases I and II, respectively (see Fig. 6b). It is noteworthy that in the case I the difference between the seasonal cycles in the different years is rather small. This result supports our most plausible interpretation of the strong seasonal differences in the trends in the NO_2 columns. In the case II, however, the seasonal variation in the NO_x emission has significantly increased from 1997 to 2007. In view of the strong difference between the trends in NO_2 columns in winter and summer, this result is consistent with the assumption underlying the case II (see Sect. 3) that the biogenic emissions behave similar to anthropogenic emissions.

The derived seasonal variations in anthropogenic emissions reflect the fact that the seasonal changes in the simulated NO_2 columns obtained with constant anthropogenic emissions is considerably smaller than the seasonal changes in the measured NO_2 columns (see Fig. 6a). In particular, the seasonal changes in the NO_x lifetime account only for about half of the strong seasonal changes in the measured NO_2 columns. The other half is interpreted here to be due to seasonal changes in total NO_x emissions. Our base case estimates of the ratios of the maximum and minimum monthly anthropogenic emissions in China are much larger than available estimates of the similar ratios based on the bottom-up inventories. Specifically, the ratio of total anthropogenic emissions in China in December to emissions in July is of 1.3 according to Zhang et al. (2007) and of 1.2 according to an earlier study (based on similar statistical data) by Streets et al. (2003). Somewhat larger maximum monthly ratios are derived for fuel combustion emissions in East Asia by Jaeglé et al. (2005, Fig. 6c) ($\sim$ 1.5) and for total emissions

ACPD
13, 255–309, 2013

(including biogenic soil emissions) for a northern China region by Wang et al. (2007, Fig. 7a) (~ 2.1) from the GOME NO_2 data using the GEOS-CHEM global chemistry transport model for estimation of the NO_x lifetime.

Note that our case II estimates are much more similar to the estimates by Wang et al. (2007, Fig. 7a) than our case I estimates. This could be expected because the case II effectively addresses the estimates of the seasonal cycle in total (anthropogenic plus biogenic) NO_x emissions which were evaluated by Wang et al. (2007). The wintertime maximum in the total NO_x emissions should indeed be less pronounced than that in anthropogenic emissions, because biogenic (microbial) emissions in China have a distinctive maximum a summer. We cannot exclude, however, that the seasonal variation of the anthropogenic NO_x emissions in our case I estimation may be overestimated due to some unidentified systematic overestimation of the background NO_2 columns (e.g. due to overestimated biogenic NO_x emissions) in the model or underestimation of the tropospheric NO_2 columns in the measurements. As explained above, we try to ensure that the main results of this study are sufficiently robust by considering simultaneously three different variants of our estimation procedure.

Our results concerning multiannual changes in NO_x emissions in China are qualitatively consistent with the results of earlier studies involving analysis of multi-annual satellite measurements over China. In particular, an accelerating and rapid growth of NO_2 column amounts over China in the late 1990s–early 2000s was found by Richter et al. (2005), He et al. (2007) and Zhang et al. (2007). Quantitative comparison of results of the different studies is however difficult because of differences in areas and periods considered, as well as in methods of trend evaluation. It is noteworthy that Zhang et al. (2007) compared satellite measurements of tropospheric NO_2 columns with data of an original emission inventory which is based on results of a reanalysis of combustion sources and an improved "dynamic" methodology allowing for changes in both activities and emission factors. Their inventory data (which unfortunately were not available for this study in a numeric format) manifest larger changes in an central eastern China region over the period from 1996 to 2001 (~ 12 percent) than the EDGAR

ACPD
13, 255–309, 2013

v4.2 and GCP data considered here, but those changes are still much smaller than the corresponding changes in the NO_2 columns derived from GOME measurements (~ 31 percent).

4.2 Analysis of nonlinear features of the multiannual emission trends

A prominent feature of the time series of the bottom-up CO_2 emission estimates is the mentioned above sharp bend in the period from 2000 to 2002. Visually, this feature underlines the existence of the two different regimes of CO_2 emission evolution in China: the first regime is associated with a neutral/slightly-decreasing CO_2 emission trend, while the second regime corresponds to a strongly positive and almost linear trend. Such different regimes should likely be associated with some fundamental changes in economic activities. Although our results confirm that the CO_2 emission trend was accelerating in China during the considered period, the difference between the trends in the periods 1996–2001 and 2001–2008 in the case of the top-down estimates is much smaller than that in the case of the bottom-up estimates.

The considerable difference in the behaviors of the top-down vs. the bottom-up CO_2 emission estimates is further demonstrated in Fig. 7. Specifically, we have again fitted our estimates and the EDGAR v4.2 data with exponential curves but this time without splitting the whole period 1996–2008 into two stages. As criteria of the goodness of the fits, we considered (i) the uncertainty of the coefficient k (see Sect. 3) and (ii) the sum of squares of deviations of logarithms of the fitted data from the corresponding fits, SS_{log}. The obtained exponential fits are shown in Fig. 7. Both the criteria indicate that the dynamics of our "top-down" emission estimates is much better consistent with a smooth exponential trend than the behavior of the EDGAR data. In other words, these results show that in agreement with a simple visual inspection of the time series of our estimates the relative rate of emission changes is accelerating much more smoothly in the case of the satellite based emission estimates than in the case of the emission inventory data between 2000 and 2002. Therefore, we can conclude that the existence

ACPD
13, 255–309, 2013

of the discussed sharp bend in emission time series is not corroborated by satellite measurements.

The origin of the strong nonlinearity in the CO_2 and NO_x emission trends found in the emission inventory data can be better understood after considering the dynamics of individual sectors of the EDGAR v4.2 emissions for China. The total anthropogenic CO and NO_x emissions for China and relative fractions of the emission sectors are presented in Fig. 8 as a function of time. It is evident that according to EDGAR v4.2 the dominant sectors (at least since 2003) providing up to about 70 (80) percent of the total CO_2 (NO_x) emissions in China are the sectors "Public Electricity and Heat Production" (PEHP) and "Manufacturing Industries and Construction" (MIC), although the "Residential and other sectors" also provide an important contribution to the CO_2 emissions. Considering the dynamics of the normalized emissions in the most important sectors, we find that the quasi neutral CO_2 and NO_x emission trends in the period from 1996 to 2001 are due to compensation of the growth of emissions in the PEHP sector by the decrease of emissions in the MIC sector. After 2001, there is an acceleration of the growth in the PEHP sector, and an upward tendency appears also in the MIC sector. The combined result of these changes is the appearance of the sharp bend of the total CO_2 and NO_x emissions in the period from 2001 to 2002. Importantly, the dynamics of both CO_2 and NO_x emissions in the major sectors looks very similar. This fact explains the similarity of the evolution of the total CO_2 and NO_x emissions in the considered period (see Fig. 2) and justifies using measurement based information on NO_x emissions for evaluating changes in CO_2 emissions.

We can conclude that if the contributions of the PEHP and MIC sectors to the total emissions from China are indeed predominant, then our estimates presented above can be considered as evidence that the acceleration of emission changes in these sectors in the period from 2000 to 2002 was much smaller than suggested by the emission inventories. One reason can be found in the activity data, which are for NO_x and CO_2 mainly coming from international energy statistics. It is commonly seen that fuel statistics do not capture rapid changes, but suffer a short time lag, in particular in case of fuel

ACPD
13, 255–309, 2013

shifts, which happened with residual fuel oil to bituminous coal in the Chinese cement production sector. At the same time, our results presented in the previous section confirm that the rates of emission changes in periods from 1996 to 2001 and from 2001 to 2008 were indeed significantly different, as it is indicated by all of the considered emission inventories.

4.3 Analysis of the spatial structure of the long-term emission changes

The results presented in the previous section address changes of emissions in China on the national scale. Taking into account previous studies it seems reasonable to expect that due to the short atmospheric lifetime of NO_2, satellite measurements of tropospheric NO_2 columns can reflect the changes of NO_2 (and, correspondingly, CO_2) emissions on even finer regional scales. Specifically, we performed estimation of the CO_2 and NO_x emissions changes using Eq. (7) but separately for different Chinese provinces. Spatial aggregation of our emission estimates on the provincial level gives us an opportunity to use for comparison the province-averaged data of the PKU-CO2 inventory. Rather than evaluating emission trends (which is impossible to do with the PKU-CO2 data available only for three years for this study), we have estimated the ratios of emission changes for the pairs of years 2008/2002 and 2002/1997. To reduce the random uncertainties, the top-down estimates were preliminary averaged over three consecutive years around the indicated years. That is, to get a more reliable estimate for, e.g. the year 2008, we have averaged the annual emission estimates over the years 2007, 2008 and 2009.

The magnitudes of the ratios of the top-down CO_2 emission estimates in the year 2008 to those in 2002 are presented in Fig. 9 and also plotted in Fig. 10 versus the similar ratios calculated with the EDGAR v4.2 and PKU-CO2 inventories. The scatterplots are presented separately for the two subsets of provinces depicted in Fig. 3. The first subset of provinces (see Fig. 3a) has been considered above. The provinces in the second subset feature considerably larger threshold magnitudes of

ACPD
13, 255–309, 2013

mean NO_2 columns ($[NO_2]_c = 5 \times 10^{15}$ molecules cm^{-2}) than the first subset ($[NO_2]_c = 1 \times 10^{15}$ molecules cm^{-2}).

It is evident that any positive correlation between our estimates of the emission ratios for the years 2008/2002, and the EDGAR v4.2 data ratio is absent. Negligible or negative correlation takes place also between the EDGAR and PKU-CO2 data. These results reflect the facts that according to EDGAR v4.2 the spatial distribution of the emission changes is almost constant over these six years, while both our top-down estimates and the PKU-CO2 bottom-up data for different provinces are rather inhomogeneous (see Fig. 9). Note that the distribution of the EDGAR v4.2 emission data is performed with sector-specific spatial proxy datasets that are kept constant over time. As such, Fig. 9b visualizes only the impact of relative change in share of the different sectors, but not yet any urbanization process which might explain the spatial inhomogeneity of the emission changes. The agreement of our estimates with the PKU-CO2 data is noticeably better (although yet far from perfect). Specifically, the correlation coefficient (r) is of 0.23 and 0.46 for the first and second subsets of provinces (with the number of provinces included being 28 and 14), respectively. A likely explanation of the larger correlation coefficient for the smaller subset of highly polluted provinces is that smaller magnitudes of NO_2 columns are associated with larger relative uncertainties caused by absolute errors in the retrievals (e.g. due to a bias in estimation of a stratospheric part of the measured total NO_2 columns) and in simulations (e.g. due to uncertainties in biogenic emissions).

The fact that our estimates demonstrate much better agreement with the data of the PKU-CO2 inventory than with the EDGAR v4.2 inventory may be considered as indication that they are sufficiently reasonable. Indeed, if our estimates were completely noisy, they could not manifest a considerable correlation with any independent data. On the other hand, the same fact can be considered as evidence that the spatial structure of real emission changes in the period from 2002 to 2008 is considerably better reproduced in the PKU-CO2 inventory than in the EDGAR v4.2 inventory. This result could indeed be expected because the PKU-CO2 inventory is based on detailed statistical

ACPD
13, 255–309, 2013

information for individual counties of China (thus even finer than the provincial level), while the EDGAR v4.2 inventory operates with the national fuel statistics, which are not all distributed to the point sources, but which uses proxy data for e.g. the residential sector. Interestingly, the correlation coefficient between our estimates of CO_2 emission ratios and the PKU-CO2 data increases from 0.46 to 0.52 when the conversion factors are assumed to be constant both in time and space (this case is not shown). That is, applying the conversion factors from EDGAR v4.2 reduces the correlation rather than increases it; this fact can be considered as indication of uncertainties in the conversion factors.

A similar analysis was performed for the ratio between the years 1997/2002. Results of this analysis which are not presented here do not contain any evidences that one of the emission inventories is considerably more accurate than the other over that period. Specifically, correlations with our top-down estimates were found to be almost negligible both with the PKU-CO2 and EDGAR v4.2 data. It seems unlikely that this result is due to a significantly different level of uncertainties in our top-down estimates. A more likely explanation is that both the PKU-CO2 and EDGAR v4.2 data for this period are very uncertain because of serious potential flaws in available statistical information about economic activities. Possible major errors in the statistical information used as input data for inventories of emissions in China were already discussed in previous publications (Akimoto et al., 2006; Zhang et al., 2007; Gregg et al., 2008; Guan et al., 2012).

5 Discussion

In this section, we discuss possible reasons for the disagreement between our estimates of CO_2 and NO_x emission changes and the data of the emission inventories. Obviously, such disagreement may be either due to (1) biases in our top-down emission estimates or (2) errors in the bottom-up estimates from emission inventories, or (3) uncertainties in the both kinds of estimates. Since the focus of this paper is on the

ACPD
13, 255–309, 2013

measurement based emission estimates, possible uncertainties in emission inventory data are discussed only very briefly.

Uncertainties in our top-down estimates of CO_2 emission trends may contain both random and systematic parts. The random part is evaluated above (see Fig. 4) in a standard way as the uncertainty of an exponential fit to the time series of measurement-based estimates. It includes random uncertainties in satellite data as well as cumulative uncertainties associated with any kind of random interannual fluctuations of α and C_b (see Eq. 2) in the real atmosphere which are not reproduced by our model. Systematic uncertainties may be due to biases and errors in the input satellite and model data and may also be associated with the assumptions mentioned in the previous section. In particular, our estimates may also be affected by systematic uncertainties in the conversion factor F.

Systematic uncertainties associated with inverse modeling are usually difficult or even impossible to quantify in a regular way due to their complicated character and the limited knowledge about possible contributing factors. This remark fully applies to the given inverse modeling study as well. Below we discuss possible systematic uncertainties and examine their potential impact on results of our analysis mainly in a qualitative way; any quantitative estimates provided below are rough and should be considered with caution.

Systematic uncertainties in satellite data include (1) retrieval errors due to neglected changes in optical properties of the atmosphere and the surface and (2) any other unidentified drifts in the data records (e.g. due to aging of satellite instruments). These kinds of uncertainties in the multi-annual satellite data for tropospheric NO_2 columns over China were earlier addressed by Richter et al. (2005) who argued that a possible bias introduced by these factors to the trends in NO_2 columns retrieved from the GOME measurements over China is insignificant in comparison to the magnitude of the trend in the period from 1996 to 2002. There is no evidence that this conclusion may be invalid in case of a longer time series considered in the given study.

ACPD
13, 255–309, 2013

The assumptions involved in our simple inverse modeling procedure (see Sect. 3) are based, in particular, on the experience of earlier studies exploiting satellite measurements of tropospheric NO_2 columns. This experience makes us believe that uncertainties associated with these assumptions cannot explain the strong disagreement between our estimates of CO_2 emission trends and corresponding data of emission inventories. Specifically, the assumption that the relationship between NO_x emissions and NO_2 columns is linear has been common for virtually all studies employing satellite measurements for estimation of NO_x emissions (e.g. Martin et al., 2003; Boersma et al., 2008; Konovalov et al., 2008; Lin et al., 2010; Kim et al., 2006, 2011).

To test the validity of this assumption in the specific case of the given study, we performed simulations of NO_2 columns with the CHIMERE model under different levels of anthropogenic NO_x emissions. Specifically, the baseline anthropogenic emissions were scaled with the scale factor ranging from 0.3 to 1. Such scaling represents the broad range of estimated NO_x emission changes in the period from 1996 to 2008 (see Fig. 5). It is found that although the response of the annual mean NO_2 columns over China to the NO_x emission changes is not exactly linear, the deviation of the relative changes in the anthropogenic part of the calculated NO_2 columns from the relative changes in the anthropogenic NO_x emissions was rather small (less than 11 percent). This result indicates that a probable positive relative bias introduced by chemical nonlinearities in the magnitudes of emission trends presented in Figs. 4 and 5 is unlikely to exceed 11 percent and cannot explain the differences with the bottom-up inventory data.

Note that in principle the nonlinearity of the relationship between NO_x emissions and NO_2 columns may be due to changes in the NO_x lifetime and the NO_2/NO_x partitioning, which may to some extent compensate each other. In our case, it is found that the increase of NO_x emissions is associated with faster than linear increase of NO_2 columns averaged annually due to the increase of the NO_x lifetime. The changes of the NO_2/NO_x ratio are found to be quite insignificant (less than 3 percent). These results suggest that the atmospheric photochemistry in China is, on the whole, predominantly in the so called high-NO_x regime (Sillmann, 1999).

ACPD
13, 255–309, 2013

It should be noted as a caveat that effects of chemical nonlinearities in the NO_2/NO_x relationship may be sensitive to the model grid resolution (Valin et al., 2011). For example, a considerably larger (than in this study) nonlinearity of the relationship between the NO_2 column and the NO_x emissions in China was reported by Stavrakou et al. (2008): based on global model simulations performed with a $5^\circ \times 5^\circ$ resolution (which is 25 time lower than the spatial resolution of the simulations in this study) they found that the lifetime of the NO_2 columns increases in January (by more than 10 percent) and decreases in July (by more than 25 percent) due to anthropogenic emissions changes between 1997 and 2006. Note that in principle our test results and the results by Stavrakou et al. (2008) may be different due to the differences in the treatment of the background NO_2 columns (specifically, they are excluded in our analysis but apparently not excluded in Stavrakou et al., 2008). Nonetheless, even taking the simulations by Stavrakou et al. (2008) into account, it appears that a decrease of the NO_x lifetime in winter and its increase in summer tend to compensate each other, so that the remaining bias in the derived trend in annual NO_x emissions is unlikely to exceed 15 percent.

The impact of NO_x emitted in the previous month on the NO_2 columns in the given month should be quite negligible because of the short chemical lifetime of NO_2 over China, which was estimated by Kunhikrishnana et al. (2004) to be in the range from 14 to 21 h. Similarly, the short lifetime of NO_x prevents it to be transported over large distances. Figure 1 clearly indicates that the NO_2 content over China is indeed determined mainly by national sources which are strongest in its eastern regions.

The omitted contribution of the NO_x emissions from lightning and wildfires can influence our estimates mainly through underestimation of the background level of the NO_2 content over China ($\mathbf{C}_b$). However, our analysis of seasonal cycle of NO_x emissions (see Sect. 4.1) indicates that $\mathbf{C}_b$ is already overestimated (probably due to overestimation of the biogenic emissions) especially in summer when NO_x emissions from both lightning and soil demonstrate a seasonal maximum. Therefore, the inclusion of NO_x emissions from lightning (which were recently estimated by Lin, 2012 to be about

ACPD
13, 255–309, 2013

two times smaller than soil emissions in China in 2006) and from wildfires (which, taking into account GFED3.1 (van der Werf et al., 2010) data and Lin, 2012 estimates contribute, on average, less than 10 percent to the total natural NO_x emissions) could hardly result in more accurate estimates of the NO_x and CO_2 emission trends in our case.

Any direct evidences of changes in biogenic NO_x emissions in China during the considered period are not yet available. Nonetheless, the changes in biogenic NO_x emissions are unlikely to exceed the changes in fertilizer consumption which according to the World Databank (http://databank.worldbank.org/ddp/home.do) has increased in China in the period from 2002 to 2008 (similar data for an earlier period have not been available) by about 25 percent (from 373 up to 468 kg per hectare of arable land). This is three times less than the supposed increase in anthropogenic NO_x emissions (see Fig. 2). Taking into account that according to our model results the background NO_2 content over China is more than 15 times smaller than the total NO_2 content (for annual averages), the impact of a possible trend in biogenic NO_x emissions on our estimates of changes in anthropogenic NO_x and CO_2 emissions is likely indeed rather negligible (less than 10 percent). An upper limit for the uncertainty associated with a possible trend in biogenic emissions is assessed above by means of a special case (case II) of our estimation procedure (see Figs. 4 and 5).

To examine the effect of interannual meteorological variability on our estimates of NO_x and CO_2 emission changes, we have performed an additional simulation with meteorological conditions for the year 1997. The year 1997 was chosen taking into account the ENSO precipitation index (ESPI) (Curtis and Adler, 2000) values which were predominantly positive during this year but were mostly negative during the year 2007. The ESPI index characterizes the long-term temporal variability of precipitation in the Eastern Asia region; it seems reasonable to assume that fluctuations of precipitation patterns are related to variability of atmospheric circulation driving air pollution transport processes. We found that replacing $\mathbf{C}_0$ and $\mathbf{C}_b$ calculated with the meteorology of year 2007 with those calculated with year 1997 in Eq. (7) resulted in very insignificant

ACPD
13, 255–309, 2013

changes (less than 1 percent). This test therefore confirms that the effect of interannual meteorological variability on our estimates of NO_x and CO_2 emission changes can be disregarded.

Changes in VOC emissions which are not taken into account in our simulations can affect the sensitivity of the NO_2 columns to changes of the NO_x emissions (see α in Eq. 2). A typical scenario which is in agreement with simulations performed by Konovalov et al. (2010) is that the increase in VOC emissions can lead to an increase of OH concentration and the decrease of α due to the increased rate of NO_2 conversion into HNO_3. A corresponding bias (which, in accordance to the mentioned scenario, is likely to be negative) in the NO_x/CO_2 emissions trends derived from satellite measurements is difficult to estimate not only because it may depend on VOC emission trends which are poorly known but also on the resolution of a model grid. Nonetheless, previous studies (e.g. Richter et al., 2005; Konovalov et al., 2008, 2010) indicated this bias is typically much smaller than the magnitude of the NO_x emission trend itself.

Uncertainties may also be associated with the simulated contribution of anthropogenic emissions to NO_2 columns (that is, with the estimated difference between $\mathbf{C}_0$ and $\mathbf{C}_b$) and the seasonal variation of NO_2 columns. This kind of uncertainties is especially difficult to evaluate. However, it is noteworthy that the trends in the original NO_2 columns derived from satellite measurements (see grey-blue lines in Fig. 5) are also statistically different from the trends in the emissions from the EDGAR v4.2 inventory (similar to our NO_x emission estimates) in the period from 1996 to 2002. Unless the trend in biogenic NO_x emissions is much larger than the trend in anthropogenic NO_x emissions (which is very improbable), this fact can be considered as a strong evidence that the trends in NO_x emissions in China is indeed underestimated in the EDGAR inventory in the indicated period.

Finally, large uncertainties (biases) which are however impossible to evaluate may appear in our estimates of the CO_2 emission trend due to errors in the conversion factor F. In principle, it is not quite improbable that even if the trend in NO_x emissions were strongly underestimated in the EDGAR inventory, the corresponding inventory trend in

ACPD
13, 255–309, 2013

CO_2 emissions would be quite correct. Such a situation could be, e.g. a consequence of a negative bias in the evolution of NO_x emission factors (assuming that the activity data in the inventory are correct). Although such a possibility cannot be easily dismissed, taking into account that according to EDGAR v4.2 the NO_x-to-CO_2 conversion factor was almost constant in the period from 1996 to 2002 (see Fig. 2) and that it is expected to increase as a result of technological advances reducing NO_x emissions from mobile sources (e.g. Zhang et al., 2007), it seems more probable that a bias in the evolution of the NO_x emission factors is positive. Moreover, possible biases in the CO_2 and NO_x emission factors cannot explain the sharp bend in the evolution of both CO_2 and NO_x emissions between 2001 and 2003, whose existence is not supported by observational evidences.

Taking into account the arguments outlined above, we can conclude that uncertainties associated with our top-down method to infer CO_2 emissions using satellite NO_x measurements and the input data (including the CO_2 to NO_x emission factor) used in our analysis can hardly be responsible for all of the considerable differences between the top-down and bottom-up estimates of NO_x and CO_2 emission changes. In our opinion, the most plausible interpretation of at least a part of the differences between our estimates and emission inventory data is that the evolution of the activity data for China in the global emission inventories in the first half of the considered period is strongly and negatively biased and shows a time lag in the reporting of fuel consumption growths (which is common in case of a fuel shift). Specifically, as it was pointed out earlier by (Akimoto et al., 2006, Gregg et al., 2008; Guan et al., 2012), the available national energy consumption data used in emission inventories to calculate emissions from the major sectors (that is, the "Public Electricity and Heat Production" and "Manufacturing Industries and Construction") may be negatively biased due to underestimation of the coal production and consumption. A likely reason for this underestimation (as it is argued in the aforementioned papers) is that activities of an increasing number of small private enterprises dealing with coal mining and electricity generation are not properly reflected in national statistics. In particular, while a large number of

ACPD
13, 255–309, 2013

small coal mines were "officially" shut down in the late 1990ths as a result of a political campaign promoted by the Chinese government, part of them actually continued operating "illegally" (Horii and Gu, 2001). Such a situation can explain a possible underestimation of the rate of CO_2 and NO_x emission change in emission inventories in the period from 1996 to 2001. Interestingly, the highest CO_2 emission estimate provided by Guan et al. (2012) for 2008 is only insignificantly larger than the corresponding estimate provided by EDGAR v4.2. This fact can be regarded as an indication that biases in the EDGAR data with respect to our estimates (see Fig. 4) should probably be mainly attributed to the years before 2008.

A comparison of the emission inventory data with corresponding measurement based estimates, which is performed in this study, cannot identify any specific problems in the top-down emission inventory data (for example, the differences between available bottom-up and our top-down estimates of CO_2 emissions may be, in principle, either due to biases in activity data or in emission factors). Nonetheless, if the emission inventory data were perfectly accurate, then the "bottom-up" and "top-down" estimates of CO_2 emission changes would be in agreement with each other (assuming that the "top-down" estimates are also sufficiently accurate). Since it is not the case in the considered situation, our results indicate that the current multi-annual data of CO_2 and/or NO_x emission inventories for China may contain major uncertainties.

6 Summary and conclusions

This study explores the idea of verification of CO_2 emissions data by means of satellite measurements of tropospheric NO_2 column amounts. Indirect estimates of CO_2 emissions are obtained from the measurement based estimates of NO_x emissions by applying the emission factors from the EDGAR v4.2 emission inventory. Using a simple inverse modeling method, we evaluate the multiannual changes (trends) in both CO_2 and NO_x anthropogenic emissions in China in the period from 1996 to 2008. The method is based on a linear relationship between NO_x emissions and the NO_2

ACPD
13, 255–309, 2013

columns, and it involves the simulations of the "background" NO_2 content in the troposphere and of a part of the seasonal cycle of NO_2 columns, which are not related to the anthropogenic NO_x emissions in China and their seasonal variations. The simulations are performed with the CHIMERE mesoscale chemistry transport model. The multiannual trends in our "top-down" estimates of CO_2 emissions are compared with the corresponding trends calculated with the data of the "bottom-up" EDGAR v4.2 and GCP global emission inventories. The trends are evaluated by means of exponential approximations of the normalized time series of annual emissions separately in the periods from 1996 to 2001 and from 2001 to 2008. Additionally, our estimates of the multiannual CO_2 emission changes are compared with the data of the national emission inventory (PKU-CO2) developed at the Peking University.

Both the top-down and bottom-up emission estimates indicate that the rate of CO_2 emission changes in China was significantly different during the two considered periods (1996–2001 and 2001–2008). Specifically, all the CO_2 emission estimates demonstrate large positive trends for the second period, while smaller trends (slightly negative or positive) are found for the first period.

However, results of our analysis also suggest that nonlinearity of CO_2 emission changes over China is strongly exaggerated in the emission inventories. Specifically, we found no observational evidences supporting the existence of a sharp bend in the emission time series in the period from 2000 to 2002. There are also significant quantitative differences between the different kinds of the CO_2 emission estimates. In particular, while the top-down estimates exhibit a positive and statistically significant trend in the period from 1996 to 2001, the global emission inventories imply that the trend was slightly negative and statistically insignificant. In contrast, the trends in the top-down and bottom-up estimates for the period from 2001 to 2008 are quantitatively similar (taking into account the range of their uncertainties).

Along with the estimates of changes in total national CO_2 emissions in China, we considered the spatial structure of these changes. Specifically, using satellite measurements of tropospheric NO_2 we have estimated the ratios of emission changes for

ACPD
13, 255–309, 2013

the years 2008 and 2002 in individual China's provinces and compared them with corresponding ratios obtained with the EDGAR v4.2 and PKU-CO2 inventory data. The comparison has revealed that our estimates agree better with the PKU-CO2 inventory than with the EDGAR inventory. This result can be considered as evidence that the accuracy of our measurement based estimates of emission changes is at least comparable with the accuracy of the corresponding data of emission inventories. Indeed, since the PKU-CO2 inventory was elaborated using the regional (provincial) energy production and consumption statistics, it is expected to more accurately reflect the spatial structure of emissions than the EDGAR inventory which is based on total national statistical information.

Finally, we have analyzed possible reasons for the discrepancies between our estimates and the data of emission inventories and presented arguments that these discrepancies are unlikely due to possible uncertainties associated with our method and measurement data. Nonetheless, it should be kept in mind that some possible systematic biases are difficult or even impossible to evaluate. Therefore, we recommend considering our estimates with sufficient caution in the same way as the data of "traditional" emission inventories which may also be subject to potential significant uncertainties. On the other hand, our results clearly indicate that the current knowledge about CO_2 emissions in China is so far insufficiently accurate. Taking into account that possible inaccuracies in emissions from China, which has grown to become recently the largest world emitter of CO_2, have major implications for climate research and prediction, the results of our study call for further researches aimed at verification of emission inventories with various satellite and ground based measurement data and at improving available GHG emission estimates.

Acknowledgements. This study was supported by the Russian Government under the contracts No. 11.G34.31.0014, 11.G34.31.0048. I. B. Konovalov acknowledges support from the Russian Foundation for Basic Research (grant No. 11-05-91061), and M. Beekmann acknowledges support from the French PICS (Programme International de Co-operation Scientifique) grant No. 5826.

ACPD
13, 255–309, 2013

References

Akimoto, H., Ohara, T., Kurokawa J., and Horii N.: Verification of energy consumption in China during 1996–2003 by using satellite observational data, Atmos. Environ., 40, 7663–7667, 2006.

Arellano, A. F., Kasibhatla, P. S., Giglio, L., van der Werf, G. R., and Randerson, J. T.: Top-down estimates of global CO sources using MOPITT measurements, Geophys. Res. Lett., 31, L01104, doi:10.1029/2003GL018609, 2004.

Bergamaschi, P., Frankenberg, C., Meirink, J. F., Krol, M., Dentener, F., Wagner, T., Platt, U., Kaplan, J. O., Körner, S., Heimann, M., Dlugokencky, E. J., and Goede, A.: Satellite chartography of atmospheric methane from SCIAMACHY onboard ENVISAT: (II) evaluation based on inverse model simulations, J. Geophys. Res., 112, D02304, doi:10.1029/2006JD007268, 2007.

Bergamaschi, P., Frankenberg, C., Meirink, J. F., Krol, M., Villani, M. G., Houweling, S., Dentener, F., Dlugokencky, E. J., Miller, J. B., Gatti, L. V., Engel, A., and Levin, I.: Inverse modeling of global and regional CH_4 emissions using SCIAMACHY satellite retrievals, J. Geophys. Res., 114, D22301, doi:10.1029/2009JD012287, 2009.

Bessagnet B., Hodzic, A., Vautard, R., Beekmann, M., Cheinet, S., Honorè, C., Liousse, C., and Rouil, L.: Aerosol modeling with CHIMERE – preliminary evaluation at the continental scale, Atmos. Environ., 38, 2803–2817, 2004.

Boden, T. A., Marland, G., and Andres, R. J.: Global, Regional, and National Fossil-Fuel CO_2 Emissions, Carbon Dioxide Information Analysis Center, Oak Ridge National Laboratory, US Department of Energy, Oak Ridge, Tenn., USA, doi:10.3334/CDIAC/00001_V2012, available at: http://cdiac.ornl.gov/trends/emis/overview_2009, last access: 4 January 2013, 2011.

Boersma, K. F., Jacob, D. J., Bucsela, E. J., Perring, A. E., Dirksen, R., van der A, R. J., Yantosca, R. M., Park, R. J., Wenig, M. O., Bertram, T. H., and Cohen, R. C.: Validation of OMI tropospheric NO_2 observations during INTEX-B and application to constrain NO_x emissions over the eastern United States and Mexico, Atmos. Environ., 42, 4480–4497, doi:10.1016/j.atmosenv.2008.02.004, 2008.

Bovensmann, H., Burrows, J. P., Buchwitz, M., Frerick, J., Nël, S., and Rozanov, V. V: SCIAMACHY – mission objectives and measurement modes, J. Atmos. Sci., 56, 127–150, 1999.

Brioude, J., Petron, G., Frost, G. J., Ahmadov, R., Angevine, W. M., Hsie, E.-Y., Kim, S.-W., Lee, S.-H., McKeen, S. A., Trainer, M., Fehsenfeld, F. C., Holloway, J. S., Peischl, J.,

ACPD
13, 255–309, 2013

Ryerson, T. B., and Gurney, K. R.: A new inversion method to calculate emission inventories without a prior at mesoscale: application to the anthropogenic CO_2 emission from Houston, Texas, J. Geophys. Res., 117, D05312, doi:10.1029/2011JD016918, 2012.

Burrows, J. P., Weber, M., Buchwitz, M., Rozanov, V., Ladstätter-Weißenmayer, A., Richter, A., DeBeek, R., Hoogen, R., Bramstedt, K., Eichmann, K.-U., Eisinger, M., and Perner, D.: The Global Ozone Monitoring Experiment (GOME): mission concept and first scientific results, J. Atmos. Sci., 56, 151–175, 1999.

Burrows, J. P., Platt, U., and Borrell, P. (Eds.): The remote sensing of tropospheric composition from space: Series Physics of Earth and Space Environments, Springer-Verlag, Berlin–Heidelberg, Germany, 2011.

Chevallier, F., Breon, F.-M., and Rayner, P. J.: Contributing of the orbiting carbon observatory to the estimation of CO_2 sources and sinks: theoretical study in a variational data assimilation framework, J. Geophys. Res., 112, D09307, doi:10.1029/2006JD007375, 2007.

Chin, M., Rood, R. B., Lin, S.-J., Muller, J. F., and Thomspon, A. M.: Atmospheric sulfur cycle simulated in the global model GOCART: model description and global properties, J. Geophys. Res., 105, 24671–24687, doi:10.1029/2000JD900384, 2000.

Chin, M., Ginoux, S., Kinne, P., Holben, B. N., Duncan, B. N., Martin, R. V., Logan, J. A., Higurashi, A., and Nakajima, T.: Tropospheric aerosol optical thickness from the GOCART model and comparisons with satellite and sunphotometer measurements, J. Atmos. Sci., 59, 461–483, 2002.

Ciais, P., Dolman, A. J., Dargaville, R., Barrie, L., Bombelli, A., Butler, J., Canadell, P., and Moriyama, T.: Geo Carbon Strategy, Geo Secretariat Geneva, FAO, Rome, 48 pp., 2010.

Curci, G., Palmer, P. I., Kurosu, T. P., Chance, K., and Visconti, G.: Estimating European volatile organic compound emissions using satellite observations of formaldehyde from the Ozone Monitoring Instrument, Atmos. Chem. Phys., 10, 11501–11517, doi:10.5194/acp-10-11501-2010, 2010.

Curtis, S. and Adler, R.: ENSO indexes based on patterns of satellite-derived precipitation, J. Climate, 13, 2786–2793, 2000.

Dufour, G., Wittrock, F., Camredon, M., Beekmann, M., Richter, A., Aumont, B., and Burrows, J. P.: SCIAMACHY formaldehyde observations: constraint for isoprene emission estimates over Europe?, Atmos. Chem. Phys., 9, 1647–1664, doi:10.5194/acp-9-1647-2009, 2009.

ACPD
13, 255–309, 2013

EC-JRC/PBL (European Commission, Joint Research Centre/Netherlands Environmental Assessment Agency): Emission Database for Global Atmospheric Research (EDGAR), release version 4.2: available at: http://edgar.jrc.ec.europa.eu, last access: 3 January 2013, 2011.

Enting, I. G.: Inverse Problems in Atmospheric Constituents Transport, Cambridge University Press, 2002.

GCP: Ten Years of Advancing Knowledge on the Global Carbon Cycle and its Management (Authors: Lavinia Poruschi, Shobhakar Dhakal and Josep Canadell), Report No. 7, Tsukuba, 2010; available at: http://www.globalcarbonproject.org/, last access: 03 February, 2012.

Ghude, S. D., Fadnavis, S., Beig, G., Polade, S. D., and van der A, R. J.: Detection of surface emission hot spots, trends, and seasonal cycle from satellite-retrieved NO_2 over India, J. Geophys. Res., 113, D20305,doi:10.1029/2007JD009615, 2008.

Ginoux, P., Chin, M., Tegen, I., Prospero, J., Holben, B., Dubovik, O., and Lin, S.-J.: Sources and global distributions of dust aerosols simulated with the GOCART model, J. Geophys. Res., 106, 20255–20273, doi:10.1029/2000JD000053, 2001.

Gregg, J. S., Andres, R. J., and Marland, G.: China: emissions pattern of the world leader in CO_2 emissions from fossil fuel consumption and cement production, Geophys. Res. Lett., 35, L08806, doi:10.1029/2007GL032887, 2008.

Guan, D., Liu, Z., Geng, Y., Lindner, S., and Hubacek, K.: The gigatonne gap in China's carbon dioxide inventories, Nat. Clim. Change, 2, 672–675, doi:10.1038/nclimate1560, 2012.

Guenther, A. B., Jiang, X., Heald, C. L., Sakulyanontvittaya, T., Duhl, T., Emmons, L. K., and Wang, X.: The Model of Emissions of Gases and Aerosols from Nature version 2.1 (MEGAN2.1): an extended and updated framework for modeling biogenic emissions, Geosci. Model Dev., 5, 1471–1492, doi:10.5194/gmd-5-1471-2012, 2012.

He, Y., Uno, I., Wang, Z., Ohara, T., Sugimoto, N., Shimizu, A., Richter, A., and Burrows, J. P.: Variations of the increasing trend of tropospheric NO_2 over central east China during the past decade, Atmos. Environ., 41, 4865–4876, 2007.

Heald, C. L., Jacob, D. J., Jones, D. B. A., Palmer, P. I., Logan, J. A., Streets, D. G., Sachse, G. W., Gille, J. C., Hoffman, R. N., and Nehrkorn, T.: Comparative inverse analysis of satellite (MOPITT) and aircraft (TRACE-P) observations to estimate Asian sources of carbon monoxide, J. Geophys. Res., 109, D15S04, doi:10.1029/2004JD005185, 2004.

Hodzic, A. and Jimenez, J. L.: Modeling anthropogenically controlled secondary organic aerosols in a megacity: a simplified framework for global and climate models, Geosci. Model Dev., 4, 901–917, doi:10.5194/gmd-4-901-2011, 2011.

ACPD
13, 255–309, 2013

Horii, N. and Gu, S. H. (Eds.): Coal industry: development of small coal mines in market transition and its externality, in: Transformation of China's Energy Industries in Market Transition and its Prospects, Chiba Institute of Developing Economics, 23–62, 2001.

Hourdin, F., Musat, I., Bony, S., Braconnot, P., Codron, F., Dufresne, J.-L., Fairhead, L., Filiberti, M.-A., Friedlingstein, P., Grandpeix, J.-Y., Krinner, G., Levan, P., Li, Z.-X., and Lott, F.: The LMDZ4 general circulation model: climate performance and sensitivity to parametrized physics with emphasis on tropical convection, Clim. Dynam., 27, 787–813, doi:10.1007/s00382-006-0158-0, 2006.

Houweling, S., Breon, F.-M., Aben, I., Rödenbeck, C., Gloor, M., Heimann, M., and Ciais, P.: Inverse modeling of CO_2 Houweling, S., Breon, F.-M., Aben, I., Rödenbeck, C., Gloor, M., Heimann, M., and Ciais, P.: Inverse modeling of CO_2 sources and sinks using satellite data: a synthetic inter-comparison of measurement techniques and their performance as a function of space and time, Atmos. Chem. Phys., 4, 523–538, doi:10.5194/acp-4-523-2004, 2004.

Houweling, S., Aben, I., Breon, F.-M., Chevallier, F., Deutscher, N., Engelen, R., Gerbig, C., Griffith, D., Hungershoefer, K., Macatangay, R., Marshall, J., Notholt, J., Peters, W., and Serrar, S.: The importance of transport model uncertainties for the estimation of CO_2 sources and sinks using satellite measurements, Atmos. Chem. Phys., 10, 9981–9992, doi:10.5194/acp-10-9981-2010, 2010.

Huang, C., Chen, C. H., Li, L., Cheng, Z., Wang, H. L., Huang, H. Y., Streets, D. G., Wang, Y. J., Zhang, G. F., and Chen, Y. R.: Emission inventory of anthropogenic air pollutants and VOC species in the Yangtze River Delta region, China, Atmos. Chem. Phys., 11, 4105–4120, doi:10.5194/acp-11-4105-2011, 2011.

Hungershoefer, K., Breon, F.-M., Peylin, P., Chevallier, F., Rayner, P., Klonecki, A., Houweling, S., and Marshall, J.: Evaluation of various observing systems for the global monitoring of CO_2 surface fluxes, Atmos. Chem. Phys., 10, 10503–10520, doi:10.5194/acp-10-10503-2010, 2010.

IPCC: Climate change 2007: synthesis report, Contribution of Working Groups I, II and III to the Fourth Assessment Report of the Intergovernmental Panel on Climate Change, Core Writing Team, edited by: Pachauri, R. K. and Reisinger, A., IPPC, Geneva, Switzerland, 104 pp., 2007.

Jaeglé, L., Steinberger, L., Martin, R. V., and Chancec, K.: Global partitioning of NO_x sources using satellite observations: relative roles of fossil fuel combustion, biomass burning and soil emissions, Faraday Discuss., 130, 407–423, 2005.

ACPD
13, 255–309, 2013

Janssens-Maenhout, G., Dentener, F., Van Aardenne, J., Monni, S., Pagliari, V., Orlandini, L., Klimont, Z., Kurokawa, J., Akimoto, H., Ohara, T., Wankmueller, R., Battye, B., Grano, D., Zuber, A., and Keating, T.: EDGAR-HTAP: a Harmonized Gridded Air Pollution Emission Dataset Based on National Inventories, European Commission Publications Office, Ispra, Italy, EUR report No EUR 25229, 40 pp., 2012.

Kadygrov, N., Maksyutov, S., Eguchi, N., Aoki, T., Nakazawa, T., Yokota, T., and Inoue, G.: Role of simulated GOSAT total column CO_2 observations in surface CO_2 flux uncertainty reduction, J. Geophys. Res., 114, D21208, doi:10.1029/2008JD011597, 2009.

Kim, S.-W., Heckel, A., McKeen, S. A., Frost, G. J., Hsie, E.-Y., Trainer, M. K., Richter, A., Burrows, J. P., Peckham, S. E., and Grell, G. A.: Satellite-observed US power plant NO_x emission reductions and their impact on air quality, Geophys. Res. Lett., 33, L22812, doi:10.1029/2006GL027749, 2006.

Kim, S.-W., Heckel, A., Frost, G. J., Richter, A., Gleason, J., Burrows, J. P., McKeen, S., Hsie, E.-Y., Granier, C., and Trainer, M.: NO_2 columns in the western United States observed from space and simulated by a regional chemistry model and their implications for NO_x emissions, J. Geophys. Res., 114, D11301, doi:10.1029/2008JD011343, 2009.

Kim, S.-W., McKeen, S. A., Frost, G. J., Lee, S.-H., Trainer, M., Richter, A., Angevine, W. M., Atlas, E., Bianco, L., Boersma, K. F., Brioude, J., Burrows, J. P., de Gouw, J., Fried, A., Gleason, J., Hilboll, A., Mellqvist, J., Peischl, J., Richter, D., Rivera, C., Ryerson, T., te Lintel Hekkert, S., Walega, J., Warneke, C., Weibring, P., and Williams, E.: Evaluations of NO_x and highly reactive VOC emission inventories in Texas and their implications for ozone plume simulations during the Texas Air Quality Study 2006, Atmos. Chem. Phys., 11, 11361–11386, doi:10.5194/acp-11-11361-2011, 2011.

Konovalov, I. B., Beekmann, M., Vautard, R., Burrows, J. P., Richter, A., Nüß, H., and Elansky, N.: Comparison and evaluation of modelled and GOME measurement derived tropospheric NO_2 columns over Western and Eastern Europe, Atmos. Chem. Phys., 5, 169-190, doi:10.5194/acp-5-169-2005, 2005.

Konovalov, I. B., Beekmann, M., Richter, A., and Burrows, J. P.: Inverse modelling of the spatial distribution of NO_x emissions on a continental scale using satellite data, Atmos. Chem. Phys., 6, 1747–1770, doi:10.5194/acp-6-1747-2006, 2006.

Konovalov, I. B., Beekmann, M., Burrows, J. P., and Richter, A.: Satellite measurement based estimates of decadal changes in European nitrogen oxides emissions, Atmos. Chem. Phys., 8, 2623-2641, doi:10.5194/acp-8-2623-2008, 2008.

ACPD
13, 255–309, 2013

Konovalov, I. B., Beekmann, M., Richter, A., Burrows, J. P., and Hilboll, A.: Multi-annual changes of NO_x emissions in megacity regions: nonlinear trend analysis of satellite measurement based estimates, Atmos. Chem. Phys., 10, 8481–8498, doi:10.5194/acp-10-8481-2010, 2010.

Kopacz, M., Jacob, D. J., Fisher, J. A., Logan, J. A., Zhang, L., Megretskaia, I. A., Yantosca, R. M., Singh, K., Henze, D. K., Burrows, J. P., Buchwitz, M., Khlystova, I., McMillan, W. W., Gille, J. C., Edwards, D. P., Eldering, A., Thouret, V., and Nedelec, P.: Global estimates of CO sources with high resolution by adjoint inversion of multiple satellite datasets (MOPITT, AIRS, SCIAMACHY, TES), Atmos. Chem. Phys., 10, 855–876, doi:10.5194/acp-10-855-2010, 2010.

Kurokawa, J., Yumimoto, K., Uno, I., and Ohara, T.: Adjoint inverse modeling of NO_x emissions over eastern China using satellite observations of NO_2 vertical column densities, Atmos. Environ., 43, 1878–1887, 2009.

Kunhikrishnana, T., Lawrencea, M. G., von Kuhlmanna, R., Richter, A., Ladstätter-Weißenmayer, A., and Burrows, J. P.: Analysis of tropospheric NO_x over Asia using the model of atmospheric transport and chemistry (MATCH-MPIC) and GOME-satellite observations, Atmos. Environ., 38, 581–596, 2004

Lee, C., Martin, R. V., van Donkelaar, A., Lee, H., Dickerson, R. R., Hains, J. C., Krotkov, N., Richter, A., Vinnikov, K., and Schwab, J. J.: SO_2 emissions and lifetimes: Estimates from inverse modeling using in situ and global, space-based (SCIAMACHY and OMI) observations, J. Geophys. Res., 116, D06304, doi:10.1029/2010JD014758, 2011.

Lin, J.-T.: Satellite constraint for emissions of nitrogen oxides from anthropogenic, lightning and soil sources over East China on a high-resolution grid, Atmos. Chem. Phys., 12, 2881–2898, doi:10.5194/acp-12-2881-2012, 2012.

Lin, J.-T., McElroy, M. B., and Boersma, K. F.: Constraint of anthropogenic NO_x emissions in China from different sectors: a new methodology using multiple satellite retrievals, Atmos. Chem. Phys., 10, 63–78, doi:10.5194/acp-10-63-2010, 2010.

Lott, F., Fairhead, L., Hourdin, F., and Levan, P.: The stratospheric version of LMDz: dynamical climatologies, arctic oscillation, and impact on the surface climate, Clim. Dynam., 25, 851–868, 2005.

Ma, J., Richter, A., Burrows, J. P., Nüß, H., and van Aardenne, J. A.: Comparison of model-simulated tropospheric NO_2 over China with GOME-satellite data, Atmos. Environ., 40, 593–604, 2006

ACPD
13, 255–309, 2013

Martin, R. V., Jacob, D. J., Chance, K., Kurosu, T., Palmer, P. I., and Evans, M. J.: Global inventory of nitrogen oxide emissions constrained by space-based observations of NO_2 columns, J. Geophys. Res., 108, 4537, doi:10.1029/2003JD003453, 2003.

Millet, D. B., Jacob, D. J., Boersma, K. F., Fu, T., Kurosu, T. P., Chance, K., Heald, C. L., and Guenther, A.: Spatial distribution of isoprene emissions from North America derived from formaldehyde column measurements by the OMI satellite sensor, J. Geophys. Res., 113, D02307, doi:10.1029/2007JD008950, 2008.

Miyazaki, K., Eskes, H. J., and Sudo, K.: Global NO_x emission estimates derived from an assimilation of OMI tropospheric NO_2 columns, Atmos. Chem. Phys., 12, 2263-2288, doi:10.5194/acp-12-2263-2012, 2012.

Monteil, G., Houweling, S., Dlugockenky, E. J., Maenhout, G., Vaughn, B. H., White, J. W. C., and Rockmann, T.: Interpreting methane variations in the past two decades using measurements of CH_4 mixing ratio and isotopic composition, Atmos. Chem. Phys., 11, 9141–9153, doi:10.5194/acp-11-9141-2011, 2011.

Müller, J.-F. and Stavrakou, T.: Inversion of CO and NO_x emissions using the adjoint of the IMAGES model, Atmos. Chem. Phys., 5, 1157–1186, doi:10.5194/acp-5-1157-2005, 2005.

Napelenok, S. L., Pinder, R. W., Gilliland, A. B., and Martin, R. V.: A method for evaluating spatially-resolved NO_x emissions using Kalman filter inversion, direct sensitivities, and space-based NO_2 observations, Atmos. Chem. Phys., 8, 5603–5614, doi:10.5194/acp-8-5603-2008, 2008.

Nassar, R., Jones, D. B. A., Kulawik, S. S., Worden, J. R., Bowman, K. W., Andres, R. J., Suntharalingam, P., Chen, J. M., Brenninkmeijer, C. A. M., Schuck, T. J., Conway, T. J., and Worthy, D. E.: Inverse modeling of CO_2 sources and sinks using satellite observations of CO_2 from TES and surface flask measurements, Atmos. Chem. Phys., 11, 6029–6047, doi:10.5194/acp-11-6029-2011, 2011.

Nüß, J. H.: An improved tropospheric NO_2 retrieval for GOME and SCIAMACHY, PhD Thesis, University of Bremen, Germany, 2005.

Ohara, T., Akimoto, H., Kurokawa, J., Horii, N., Yamaji, K., Yan, X., and Hayasaka, T.: An Asian emission inventory of anthropogenic emission sources for the period 1980–2020, Atmos. Chem. Phys., 7, 4419–4444, doi:10.5194/acp-7-4419-2007, 2007.

Olivier, J. G. J., Berdowski, J. J. M., Peters, J. A. H. W., Bakker, J., Visschedijk, A. J. H., and en Bloos, J.-P. J.: Applications of EDGA R. Including a description of EDGAR 3.0: reference

ACPD
13, 255–309, 2013

database with trend data for 1970–1995, RIVM, Bilthoven, RIVM report No 773301 001/ NOP report No 410200 051, 142 pp., 2001.
Olivier, J. G. J., Van Aardenne, J. A., Dentener, F., Pagliari, V., Ganzeveld, L. N. and Peters, J. A. H. W.: Recent trends in global greenhouse gas emissions: regional trends 1970–2000 and spatial distribution of key sources in 2000, Environ. Sci., 2, 81–99, doi:10.1080/15693430500400345, 2005.
Pak, B. C. and Prather, M. J.: CO_2 source inversion using satellite observations in the upper troposphere, Geophys. Res. Lett., 28, 4571–4574, 2001.
Palmer, P. I., Jacob, D. J., Fiore, A. M., and Martin, R. V.: Mapping isoprene emissions over North America using formaldehyde column observations from space, J. Geophys. Res., 108, 4180, doi:10.1029/2002JD002153, 2003.
Palmer, P. I., Suntharalingam, P., Jones, D. B. A., Jacob, D. J., Streets, D. G., Fu, Q. Y., Vay, S. A., and Sachse, G. W.: Using CO_2:CO correlations to improve inverse analyses of carbon fluxes, J. Geophys. Res., 111, D12318, doi:10.1029/2005JD006697, 2006.
Pétron, G., Granier, C., Khattatov, B., Yudin, V., Lamarque J. F., Emmons, L., Gille, J., and Edwards, D. P.: Monthly CO surface sources inventory based on the 2000–2001 MOPITT satellite data, Geophys. Res. Lett., 31, L21107, doi:10.1029/2004GL020560, 2004.
Rayner, P. J. and O'Brien, D. M.: The utility of remotely sensed CO_2 concentration data in surface source inversions, Geophys. Res. Lett., 28, 175–178, 2001.
Richter, A., Burrows, J. P., Nüß, H., Granier, C., and Niemeier, U.: Increase in tropospheric nitrogen dioxide over China observed from space, Nature, 437, 129–132, doi:10.1038/nature04092, 2005.
Rivier, L., Ciais, P., Hauglustaine, D. A., Bakwin, P., Bousquet, P., Peylin, P., and Klonecki, A.: Evaluation of SF_6, C_2Cl_2, and CO to approximate fossil fuel CO_2 in the Northern Hemisphere using a chemistry transport model, J. Geophys. Res., 111, D16311, doi:10.1029/2005JD006725, 2006.
Schmidt, H., Derognat, C., Vautard, R., and Beekmann, M.: A comparison of simulated and observed ozone mixing ratios for the summer of 1998 in Western Europe, Atmos. Environ., 36, 6277–6297, 2001
Schulze, E.-D., Luyssaert, S., Ciais, P., Freibauer, A., Janssens, I. A., Soussana, J. F., Smith, P., Grace, J., Levin, I., Thiruchittampalam, B., Heimann, M., Dolman, A. J., Valentini, R., Bousquet, P., Peylin, P., Peters, W., Rödenbeck, C., Etiope, G., Vuichard, N., Wattenbach, M., Nabuurs, G. J., Poussi, Z., Nieschulze, J., Gash, J. H., and the CarboEurope Team:

ACPD
13, 255–309, 2013

Importance of methane and nitrous oxide for Europe's terrestrial greenhouse gas balance, Nat. Geosci., 2, 842–850, 2009.
Sillmann, S.: The relation between ozone, NO_x and hydrocarbons in urban and polluted rural environments, Atmos. Environ., 33, 1821–1845, 1999.
Skamarock, W. C., Klemp, J. B., Dudhia, J., Gill, D. O., Barker, D. M., Wang, W., and Powers, J. G.: A description of the Advanced Research WRF Version 2, NCAR Tech Notes-468+STR, 2005.
Stavrakou, T., Müller, J.-F., Boersma, K. F., De Smedt, I., and van der A, R. J.: Assessing the distribution and growth rates of NO_x emission sources by inverting a 10-year record of NO_2 satellite columns, Geophys. Res. Lett., 35, L10801, doi:10.1029/2008GL033521, 2008.
Stavrakou, T., Müller, J.-F., De Smedt, I., Van Roozendael, M., Kanakidou, M., Vrekoussis, M., Wittrock, F., Richter, A., and Burrows, J. P.: The continental source of glyoxal estimated by the synergistic use of spaceborne measurements and inverse modelling, Atmos. Chem. Phys., 9, 8431–8446, doi:10.5194/acp-9-8431-2009, 2009.
Streets, D. G., Bond, T. C., Carmichael, G. R., Fernandes, S. D., Fu, Q., He, D., Klimont, Z., Nelson, S. M., Tsai, N. Y., Wang, M. Q., Woo, J.-H., and Yarber, K. F.: An inventory of gaseous and primary aerosol emissions in Asia in the year 2000, J. Geophys. Res., 108, 8809, doi:10.1029/2002JD003093, 2003.
Suntharalingam, P., Jacob, D. J., Palmer, P. I., Logan, J. A., Yantosca, R. M., Xiao, Y., Evans, M. J., Streets, D. G., Vay, S. L., and Sachse, G. W.: Improved quantification of Chinese carbon fluxes using CO_2/CO correlations in Asian outflow, J. Geophys. Res., 109, D18S18, doi:10.1029/2003JD004362, 2004.
van der Werf, G. R., Randerson, J. T., Giglio, L., Collatz, G. J., Mu, M., Kasibhatla, P. S., Morton, D. C., DeFries, R. R., Jin, Y., and van Leeuwen, T. T.: Global fire emissions and the contribution of deforestation, savanna, forest, agricultural, and peat fires (1997–2009), Atmos. Chem. Phys., 10, 11707–11735, doi:10.5194/acp-10-11707-2010, 2010.
Valin, L. C., Russell, A. R., Hudman, R. C., and Cohen, R. C.: Effects of model resolution on the interpretation of satellite NO_2 observations, Atmos. Chem. Phys., 11, 11647–11655, doi:10.5194/acp-11-11647-2011, 2011.
Wang, R., Tao, S., Ciais, P., Shen, H. Z., Huang, Y., Chen, H., Shen, G. F., Wang, B., Li, W., Zhang, Y. Y., Lu, Y., Zhu, D., Chen, Y. C., Liu, X. P., Wang, W. T., Wang, X. L., Liu, W. X., Li, B. G., and Piao, S. L.: High resolution mapping of combustion processes and implications

ACPD
13, 255–309, 2013

for CO_2 emissions, Atmos. Chem. Phys. Discuss., 12, 21211–21239, doi:10.5194/acpd-12-21211-2012, 2012.

Wang, S. W., Streets, D. G., Zhang, Q., He, K. B., Chen, D., Kang, S. C., Lu, Z. F., and Wang, Y. X.: Satellite detection and model verification of NO_x emissions from power plants in Northern China, Environ. Res. Lett., 5, 044007, doi:10.1088/1748-9326/5/4/044007, 2010.

Wang, S. W., Zhang, Q., Streets, D. G., He, K. B., Martin, R. V., Lamsal, L. N., Chen, D., Lei, Y., and Lu, Z.: Growth in NO_x emissions from power plants in China: bottom-up estimates and satellite observations, Atmos. Chem. Phys., 12, 4429–4447, doi:10.5194/acp-12-4429-2012, 2012.

Wang, Y., McElroy, M. B., Martin, R. V., Streets, D. G., Zhang, Q., and Fu, T.-M.: Seasonal variability of NO_x emissions over east China constrained by satellite observations: Implications for combustion and microbial sources, J. Geophys. Res., 112, D06301, doi:10.1029/2006JD007538, 2007.

Wicker, L. J. and Skamarock, W. C.: Time splitting methods for elastic models using forward time schemes, Mon. Weather Rev., 130, 2088–2097, 2002.

Zhang, Q., Streets, D. G., He, K., Wang, Y., Richter, A., Burrows, J. P., Uno, I., Jang, C. J., Chen, D., Yao, Z., and Lei, Y.: NO_x emission trends for China, 1995–2004: the view from the ground and the view from space, J. Geophys. Res., 112, D22306, doi:10.1029/2007JD008684, 2007.

Zhao, B., Wang, P., Ma, J. Z., Zhu, S., Pozzer, A., and Li, W.: A high-resolution emission inventory of primary pollutants for the Huabei region, China, Atmos. Chem. Phys., 12, 481–501, doi:10.5194/acp-12-481-2012, 2012.

ACPD
13, 255–309, 2013

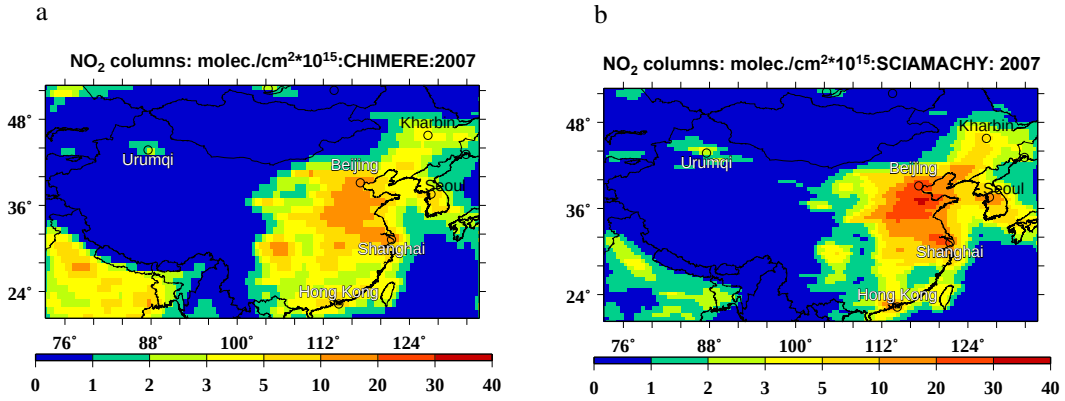

Fig. 1. Annual mean tropospheric NO_2 column amounts (molecules $\times 10^{15}$ cm^{-2}) simulated with the CHIMERE model **(a)** and derived from SCIAMACHY measurements **(b)** for the year 2007.

ACPD
13, 255–309, 2013

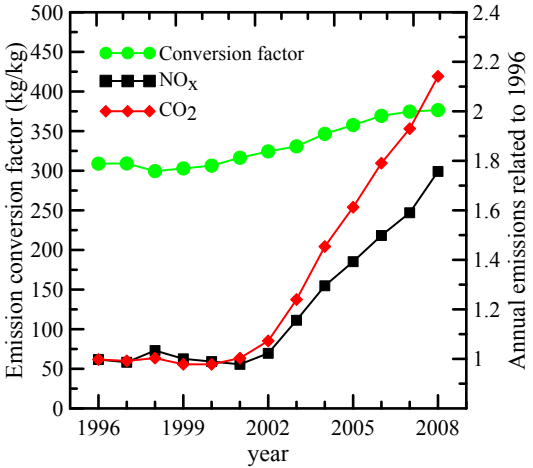

Fig. 2. Multiannual evolution of the CO_2 and NO_x anthropogenic emissions in China and the behavior of the corresponding NO_x-to-CO_2 emission conversion factor F (see Eq. 6) according to the EDGAR v4.2 emission inventory. The emissions are normalized to their values in 1996.

ACPD
13, 255–309, 2013

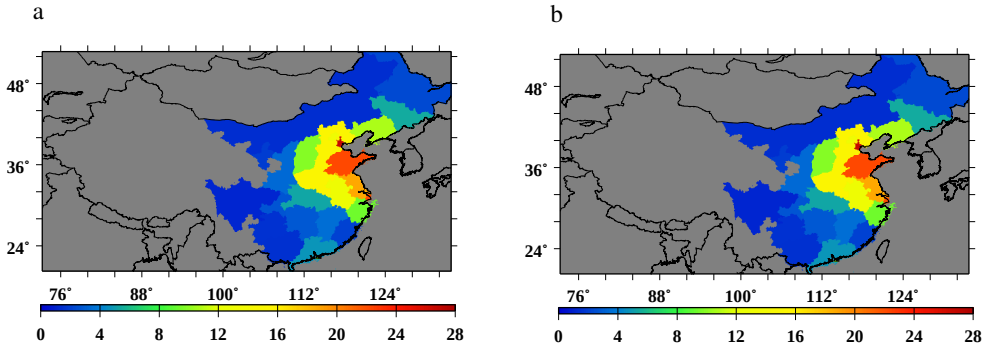

Fig. 3. The provinces of China taken into account in the analysis of the spatial distribution of emission changes for different threshold levels, $[NO_2]_c$, of the (depicted in the plots) annual mean measured tropospheric NO_2 column amounts for year 2008: **(a)** $[NO_2]_c = 1 \times 10^{15}$ molecules cm^{-2} and **(b)** $[NO_2]_c = 5 \times 10^{15}$ molecules cm^{-2}.

ACPD
13, 255–309, 2013

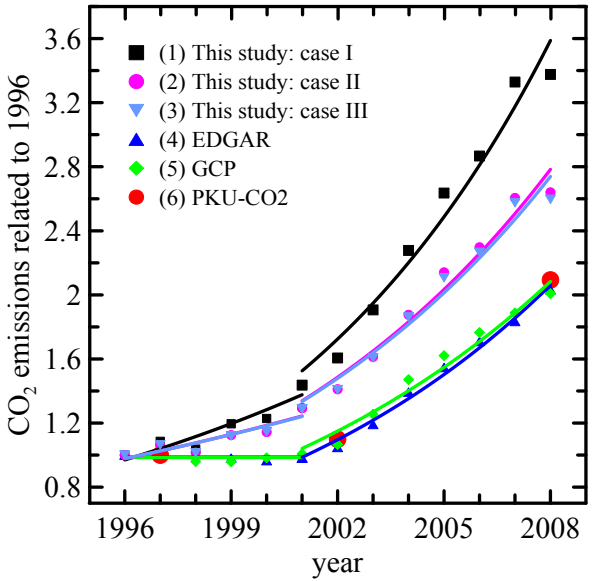

Fig. 4. Multiannual exponential total anthropogenic CO_2 emission trends in China derived from satellite measurements and calculated with the EDGAR v4.2 and GCP data for the periods from 1996 to 2001 and from 2001 to 2008. Additionally, the PKU-CO2 data are shown for three years (1997, 2002 and 2008). All the data are normalized to the values from 1996. Note that only relative changes (not absolute values) of emissions are evaluated in this study; thus the differences between the top-down and bottom-up emission estimates cannot be unambiguously attributed to certain years.

ACPD
13, 255–309, 2013

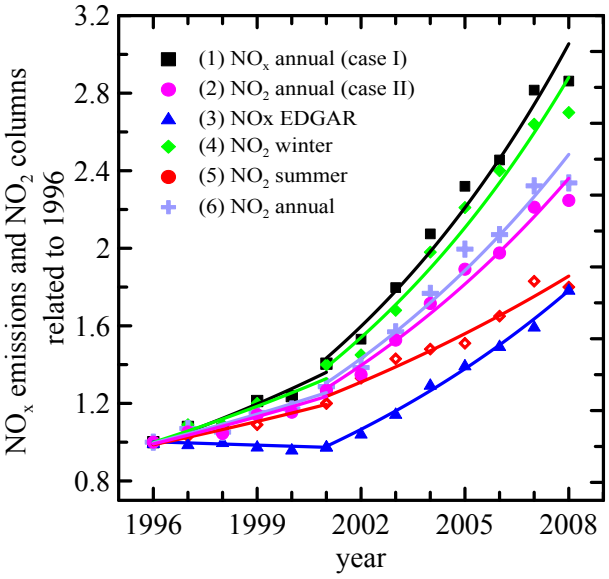

Fig. 5. Multiannual exponential NO_x emission trends (1,2) derived from satellite measurements in the cases I and II of the estimation procedure, respectively, and (3) evaluated using the EDGAR v4.2 inventory. The trends are also shown for the measured tropospheric NO_2 columns averaged seasonally for the cold (4) and warm (5) seasons, and annually (6). All the data are normalized to the values from 1996.

ACPD
13, 255–309, 2013

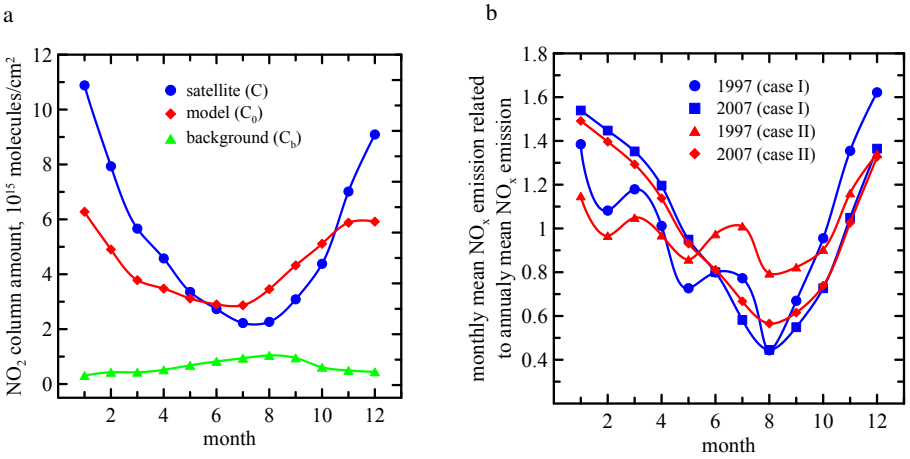

Fig. 6. The seasonal variation in NO_2 column amounts derived from satellite measurements (C) and simulated with CHIMERE with (C_0) and without anthropogenic NO_x emissions (C_b) in China **(a)** and the estimated seasonal cycle of anthropogenic NO_x emissions in 1997 and 2007 for the cases I and II of the estimation method. The NO_2 columns and NO_x emissions are averaged over the eastern China region shown in Fig. 3a. Note that C_0 are calculated without any seasonal variation in anthropogenic emissions. Note also that oscillations in the plot **(b)** are most probably due to uncertainties in the monthly emission estimates.

ACPD
13, 255–309, 2013

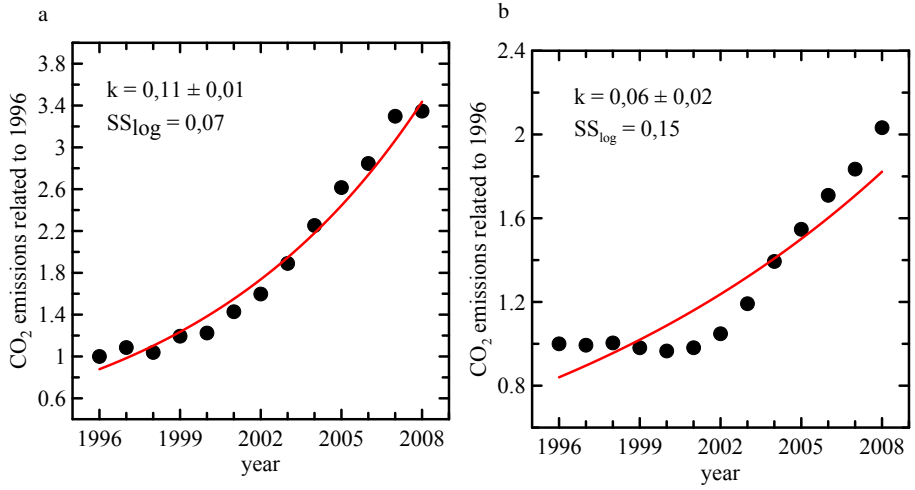

Fig. 7. Multiannual time series of the normalized CO_2 total anthropogenic emissions in China obtained from **(a)** satellite measurements and **(b)** the EDGAR v4.2 emission inventory, along with corresponding exponential approximations over the whole period from 1996 to 2008.

ACPD
13, 255–309, 2013

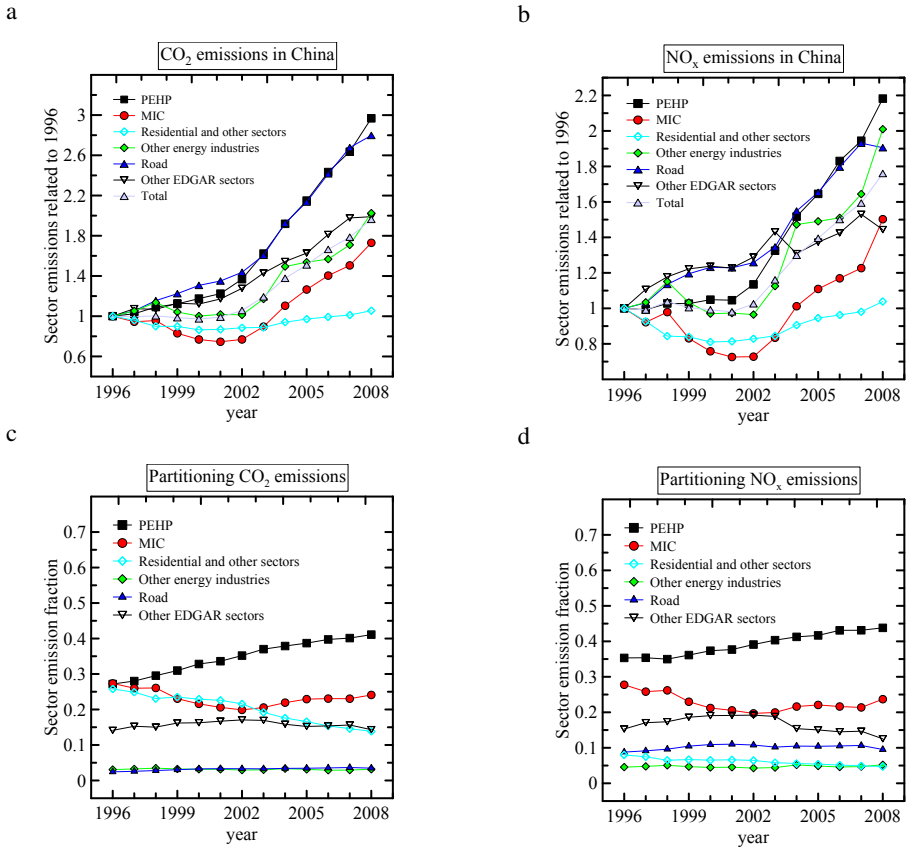

Fig. 8. The total annual anthropogenic CO_2 **(a)** and NO_x **(b)** emissions in China and their partitioning **(c, d)** among the emissions sectors according to the EDGAR v4.2 inventory. The emission data are normalized to the values from 1996. PEHP: Public Electricity and Heat Production; MIC: Manufacturing Industries and Construction.

ACPD
13, 255–309, 2013

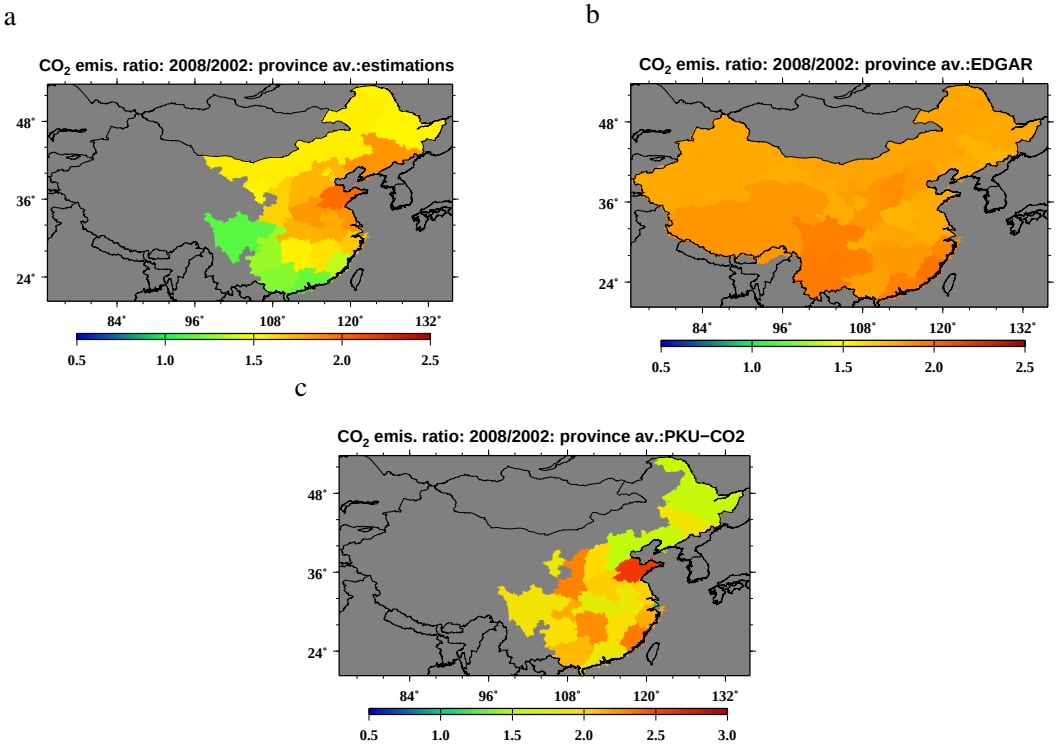

Fig. 9. Magnitudes of the ratio of the top-down satellite based CO_2 emission estimates in the year 2008 to those in 2002 **(a)** along with the similar ratios calculated with the EDGAR v4.2 **(b)** and PKU-CO2 inventories **(c)**.

ACPD
13, 255–309, 2013

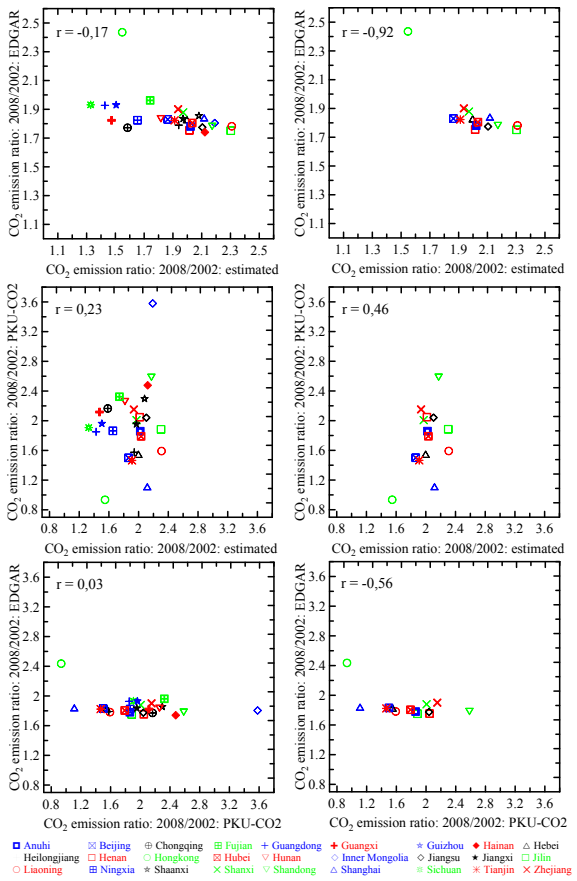

Fig. 10. Scatterplots of the ratios of different CO_2 emission estimates for the years 2008 and 2002: (left) for the eastern provinces depicted in Fig. 3a and (right) for the selected highly polluted provinces indicated in Fig. 3b.

ACPD
13, 255–309, 2013